Phytochemistry 192 (2021) 112947

Contents lists available at ScienceDirect

Phytochemistry

journal homepage: www.elsevier.com/locate/phytochem

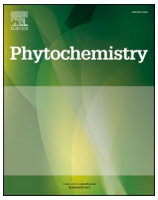

Engineering of benzoxazinoid biosynthesis in *Arabidopsis thaliana*: Metabolic and physiological challenges

Aleksej Abramov [a], Thomas Hoffmann [b], Timo D. Stark [c], Linlin Zheng [d], Stefan Lenk [d], Richard Hammerl [c], Tobias Lanzl [a], Corinna Dawid [c], Chris-Carolin Schön [a], Wilfried Schwab [b], Alfons Gierl [d], Monika Frey [a,*]

[a] Chair of Plant Breeding, Technical University of Munich, Liesel-Beckman Str. 2, 85354, Freising, Germany
[b] Associate Professorship of Biotechnology of Natural Products, Technical University of Munich, Liesel-Beckmann Str. 1, 85354, Freising, Germany
[c] Chair of Food Chemistry and Molecular Sensory Science, Technical University of Munich, Lise-Meitner Str. 34, 85354, Freising, Germany
[d] Chair of Genetics, Technical University of Munich, Emil-Ramann Str. 8, 85354, Freising, Germany

ARTICLE INFO

Keywords:
Arabidopsis thaliana (Brassicaceae)
Zea mays (Poaceae)
Benzoxazinones
Chemical defence
Indolinone
Phytotoxicity
Metabolic stress
Transgenic pathway
Bioengineering
Pathway evolution

ABSTRACT

Plant specialised metabolites constitute a layer of chemical defence. Classes of the defence compounds are often restricted to a certain taxon of plants, e.g. benzoxazinoids (BX) are characteristically detected in grasses. BXs confer wide-range defence by controlling herbivores and microbial pathogens and are allelopathic compounds. In the crops maize, wheat and rye high concentrations of BXs are synthesised at an early developmental stage. By transfer of six *Bx*-genes (*Bx1* to *Bx5* and *Bx8*) it was possible to establish the biosynthesis of 2,4-dihydroxy-1,4-benzoxazin-3-one glucoside (GDIBOA) in a concentration of up to 143 nmol/g dry weight in *Arabidopsis thaliana*. Our results indicate that inefficient channeling of substrates along the pathway and metabolisation of intermediates in host plants might be a general drawback for transgenic establishment of specialised metabolite biosynthesis pathways. As a consequence, BX levels required for defence are not obtained in Arabidopsis. We could show that indolin-2-one (ION), the first specific intermediate, is phytotoxic and is metabolised by hydroxylation and glycosylation by a wide spectrum of plants. In Arabidopsis, metabolic stress due to the enrichment of ION leads to elevated levels of salicylic acid (SA) and in addition to its intrinsic phytotoxicity, ION affects plant morphology indirectly via SA. We could show that *Bx3* has a crucial role in the evolution of the pathway, first based on its impact on flux into the pathway and, second by C3-hydroxylation of the phytotoxic ION. Thereby BX3 interferes with a supposedly generic detoxification system towards the non-specific intermediate.

1. Introduction

In the plant kingdom, specialised metabolites play an indispensable role for communication and chemical defence within the ecosystem (Hartmann, 2007). Plant defence compounds are characterised by intrinsic undirected reactivity with biological material and consequently can target a wide range of predators, such as herbivorous insects, nematodes and microbial pathogens. Distinct pathways descending from primary metabolism fuel the multitude of defensive chemical structures. This link given, any defence compound could be established in arbitrary plant species. However, in evolution classes of compounds are frequently restricted to individual plant lineages (Wink, 2003) and distinct compound classes are often characteristics of single orders or families of plants (Wink and Waterman, 1998). The established specialisation reduces the probability that generalists (e.g. herbivores) emerge in the ecosystem but exclusivity might also result from metabolic limitations. Defence chemicals of plants commonly have relatively mild toxicity and high local concentrations are needed to provide protection. Especially in the case of preformed defence compounds when pathway expression is not restricted to tissues under attack, specialised metabolites constitute a considerable sink. This constraint might be most severe if several biosyntheses use the same immediate resource. An example of mutual exclusivity is found in the genus *Hordeum* with alternative presence of gramine and benzoxazinoids which both are derived from the tryptophan biosynthesis pathway (Grün et al., 2005). The question arises whether in a plant that has an established chemical

* Corresponding author.
E-mail address: monika.frey@tum.de (M. Frey).

https://doi.org/10.1016/j.phytochem.2021.112947
Received 22 June 2021; Received in revised form 29 August 2021; Accepted 7 September 2021
Available online 15 September 2021

defence mechanism parallel expression of a second defence compound is possible in a way that pest resistance is broadened.

Several specialised defence metabolic pathways have been elucidated at the molecular level (Nützmann et al., 2016 for review) and can potentially be transferred between species transgenically. The constitutive defence metabolite dhurrin, an aromatic cyanogenic glucoside (CG) of Sorghum was transferred to *Arabidopsis thaliana* (termed Arabidopsis in the following), and the biosynthesis of the Arabidopsis intrinsic glucosinolates (GLS) was established in *Nicotiana benthamiana* (Møldrup et al., 2012). CG biosynthesis in Arabidopsis raised the lethality of the plant to the flea beetle *Phyllotreta nemorum* and reduced leaf damage (Tattersall et al., 2001). The non-host tobacco was engineered to attract the crucifer specialist insect *Plutella xylostella* for oviposition *via* transgenic GLS. Since the newly-hatched larvae cannot survive on tobacco a dead-end trap plant is generated (Møldrup et al., 2012). Hence biosynthesis transfer can be productive. GLS are characteristically found in Brassicaceae and are classified as indolic, chain elongating aromatic, and aliphatic GLS (Halkier and Gershenzon, 2006). Indolic GLS biosynthesis in Arabidopsis originates from tryptophan (TRP) and is interconnected with amino acid, auxin, and phytoalexin camalexin biosynthesis (Halkier and Gershenzon, 2006, Fig. 1). The question is whether an additional branch in such a complex network can be introduced and yield substantial amount of the alien metabolite. A potential connection to the network can be made with benzoxazinoid (BX) biosynthesis. BX are well-known broad range defence metabolites that are linked with TRP biosynthesis *via* the shared intermediate indole-3-glycerol phosphate (Fig. 1). Transgenic BX expression in Arabidopsis will integrate into the hub between amino acid, hormone and defence metabolite biosynthesis and hence will demonstrate flexibility and capacity of the host Arabidopsis for production of indolic compounds and has the potential to possibly fortify chemical defence by an addition to the arsenal.

BXs serve as preformed defence chemicals in the major crops maize, wheat and rye. In addition, BXs are also produced in individual species of unrelated dicots (Niculaes et al., 2018). The impact of BXs on plant defence, especially for the control of herbivorous insects (Klun et al., 1967) and in allelopathy (Hietala and Virtanen, 1960) was recognised in the 1960s. In maize, high BX levels have been selected in breeding programs (Klun et al., 1970). DIBOA (2,4-dihydroxy-1,4-benzoxazin-3-one) is the final product of benzoxazinoid biosynthesis in wild *Hordeum* species and is also a major metabolite in rye leaves. BXs are so-called two-component defence metabolites (Pentzold et al., 2014) that are stabilised by glucosylation and the glucosides are supposed to be stored in the vacuole (Frey et al., 2009). The complementary beta-glucosidase that releases BXs reactive aglycon is detected in plastids and is associated with the cell wall (Nikus et al., 2001). BX are present at high concentrations in seedlings (Schulz et al., 2013) and locally inducible in response to herbivore and microbial infestation in adult plants (Handrick et al., 2016; Huffaker et al., 2013). Intermediates of BX biosynthesis are rarely detectable. The biosynthetic pathway has been elucidated in maize (Frey et al., 1997; Handrick et al., 2016; Jonczyk et al., 2008; Meihls et al., 2013; von Rad et al., 2001, Fig. 1) and to a large extent in wheat, rye and *H. lechleri* (Grün et al., 2005; Nomura et al., 2005). To generate the first toxic BX, DIBOA, five genes are required. The signature enzyme BX1 initiates the pathway by using indole 3-glycerol phosphate (IGP) from primary metabolism to produce indole. BX1 is a homolog of the alpha-subunit of tryptophan synthase (TSA), and functions as an indole synthase (Fig. 1). Four genes encode the cytochrome P450 monooxygenases (P450s), BX2 to BX5, that catalyse two consecutive O-hydroxylations yielding indolin-2-one (ION), 3-hydroxy-1,3-dihydro-indol-2-one (HION), 2-hydroxy-1,4-benzoxazin-3-one (HBOA) by ring expansion and DIBOA by final N-hydroxylation (Fig. 1). P450 reactions are often essential for the genesis of bioactive compounds. Eukaryotic P450s and the P450 oxidoreductases (POR) that provide the required electrons for enzymatic reactions are anchored in the endoplasmic reticulum (ER). BX8 and BX9 represent BX-specific UGTs required for detoxification by glucosylation (von Rad et al., 2001). Hence safe BX production in heterologous hosts demands the transfer of six genes, *Bx1* to *Bx5* and *Bx8*. The functionality of the heterologously expressed *Bx* genes has been verified in yeast and *E. coli* (Frey et al., 1997; Grün et al., 2005; von Rad et al., 2001).

Here, we demonstrate the transfer of the biosynthetic pathway for the BX DIBOA-glucoside (GDIBOA) to Arabidopsis. The efficiency of biosynthesis is affected by competition with tryptophan formation for the shared intermediate, and by disturbance of the flux by chemical modification of BX intermediates. We show that pathway-specific hydroxylation of the unique signature metabolite indolin-2-one (ION) by BX3 is essential for GDIBOA production. Accumulation of ION causes metabolic stress similar to pathogen infection as expressed by changes in salicylic acid (SA) homeostasis. Both elevated SA and presence of ION influence the morphology. In Arabidopsis and potentially more general in plants ION is hydroxylated by P450s and glucosylated by promiscuous UGTs possibly by a common sequence of reactions intended to detoxify xenobiotics and allelochemicals.

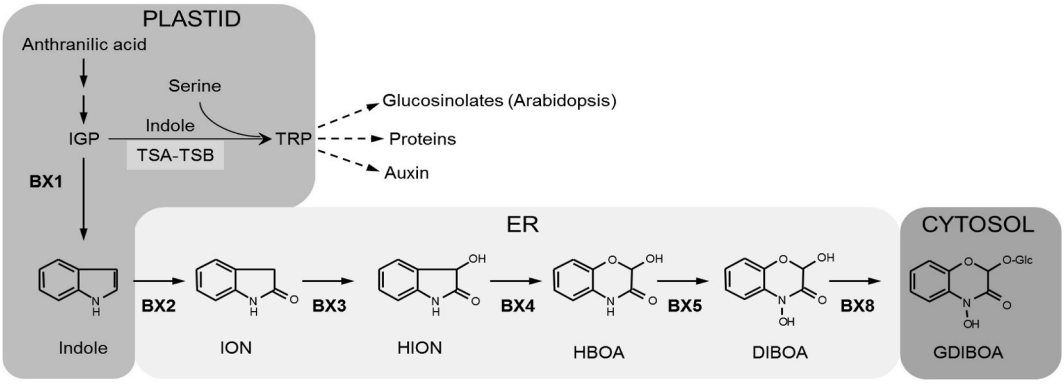

Fig. 1. Benzoxazinoid biosynthesis integration in the Arabidopsis metabolic network. BX biosynthesis is linked to the primary metabolism via the intermediate indole-2-glycerol phosphate (IGP) that is shared with the tryptophan (TRP) biosynthesis. In addition to the function as building block in protein biosynthesis TRP is a substrate in auxin biosynthesis. In Arabidopsis, TRP is additionally used for biosynthesis of constitutive (indolic glucosinolates) and induced (camalexin) defence compounds. DIBOA is the first toxic intermediate and gets stabilised by glucosylation. In the grasses further hydroxylations and methylations take place depending on developmental stage, tissue and pathogen attack. The BX enzymes and the respective products are denoted. Steps of the biosynthesis take place in the plastid, at the endoplasmic reticulum (ER) and in the cytosol.

Table 1
Nomenclature of transgenic lines. The presence of the respective transgene in homozygous (xx) or heterozygous (x) state is indicated.

Identifier	Genotype	Bx1	Bx2	Bx3	Bx4	Bx5	Bx8	ZmPor2
Bx1Bx2	*pSUR2::Bx1 p35S::Bx2*	xx	xx					
Bx1Bx2Bx3	*pSUR2::Bx1 p35S::Bx2 p35S::Bx3*	xx	xx	xx				
Cluster	*Bx2 Bx3 Bx4 Bx5*		xx	xx	xx	xx		
Cluster+	*Bx2 Bx3 Bx4 Bx5 Bx8 ZmPor2*		xx	xx	xx	xx	xx	xx
Bx1C+	*p35S::Bx1 Cluster+*	xx	xx	xx	xx	xx	xx	xx
Bx1Bx2C+	*pSUR2::Bx1 p35S::Bx2 Cluster+*	xx	xx	x	x	x	x	x
Bx1Bx3C+	*pSur2::Bx1 p35S::Bx3 Cluster+*	xx	x	xx	x	x	x	x
Bx1Bx2Bx3C+	*pSUR2::Bx1 p35S::Bx2 p35S::Bx3 Cluster+*	xx	xx	xx	x	x	x	x

2. Results

2.1. Transgenic Arabidopsis synthesises benzoxazinoids

Previous experiments to transfer GDIBOA biosynthesis to Arabidopsis by first generating individual *Bx*-gene transgenics and consecutive merging by crossing were not successful. Since in this approach the six essential genes of the pathway (Fig. 1) were driven by the cauliflower mosaic virus 35S promoter (*p35S*) gene silencing caused by the multiple use of the strong promoter might have occurred (Mlotshwa et al., 2010). To promote gene expression we employed Arabidopsis promoters and changed the codon usage of the G/C-rich maize genes to fit to the A/T preference of Arabidopsis. For the choice of promoters the criteria were moderate to high expression in rosette leaves and low expression in flower organs, the latter based on the finding that joining of *Bx1* and *Bx2* both expressed as p35 S-constructs generated female and male sterile plants (Supplemental Figure S12B). According to the Arabidopsis eFP browser developmental map (Winter et al., 2007) P450 genes of glucosinolate biosynthesis, *Cyp71B7, Cyp79B2*, *Cyp83A1*, and *Cyp83B1 (SUPERROOT2)* displayed a suitable expression pattern and the cDNA of the *Bx*-genes were integrated between the intrinsic start and stop codons (Supplemental Figure S1). To reduce the number of required transformation events, the genes *Bx2* to *Bx5* were merged in one T-DNA and the resulting transgenics were termed Cluster (the nomenclature of the transgenics is summarised Table 1). As another precautionary measure to guarantee efficiency of the maize P450s we isolated the maize gene model Zm00001d026483 that is annotated as P450 oxidoreductase (named *ZmPor2* in the following). According to the maize eFP browser (Stelpflug et al., 2016; Winter et al., 2007), *ZmPor2* is highly expressed in seedlings. In the transgenics the gene is driven by *p35S*. The enzymatic activity of P450s in the transgenics was verified with isolated microsomes (Table 2A). For the substrates ION, and HION consecutive reactions yielding HBOA and DIBOA, respectively were detected (Table 2A). By crossing and selfing we obtained transgenic plants that feature in addition to the *Cluster* genes the UDPG: DI(M)BOA-glucosyltransferase *Bx8* and *ZmPor2*, each transgene homozygously (Cluster+, Table 1). To complete the pathway Cluster + plants were crossed with transgenics harbouring *Bx1* driven by promoters conferring different levels of expression, the strong promoters *p35S* and *pSUR2* and the weak promoter *pNos* (Supplemental Figure S2A). We could verify GDIBOA biosynthesis in Arabidopsis when *Bx1* was driven by *pSUR2* or *p35S*. Quantification by LC-MS revealed concentrations of 3.7±0.7 nmol GDIBOA/g DW (Table 3) for *p35S::Bx1Cluster+* (Bx1C+) and *pSUR2::Bx1Cluster* + plants. The result shows that high levels of BX1 are required to initiate BX biosynthesis. The concentrations achieved in the transgenics however are far below the level reached in grasses (e.g. up to 20 000 nmol/g DW in rye leaves, Copaja et al., 2006; Rice et al., 2005) and also below the effective concentration for defence (1 μmol/g FW; Bravo et al., 1997; Bravo and Lazo, 1996; Campos et al., 1989; Long et al., 1975).

2.2. Inefficient channelling of the pathway and metabolisation of intermediates is a major constraint for efficient BX biosynthesis

In contrast to the *in vitro* assay with isolated microsomes in feeding experiments compounds are modified in the network of all enzymes present in a cell. Hence, feeding with indole resulted in a significant increase of TRP, independent of the line analysed. In addition, the metabolite profiles of Cluster + transgenics after feeding of the substrates of the biosynthetic pathway (Table 2B) revealed the presence of unknown metabolites that might represent chemically modified intermediates of BX biosynthesis. Cluster + feeding with HION and HBOA produced the expected next and consecutive compounds of the pathway (HBOA, DIBOA, GDIBOA), but additional signals were found that could be interpreted as glycosylated HBOA (Supplemental Figure S3). Interestingly, the metabolite was also present in HBOA fed Col-0 indicating the catalysis by an Arabidopsis endogenous glycosyltransferase. Likewise, both the transgenics and Col-0 contain the same metabolites after ION application and the predicted BX intermediate HION is not detectable (Table 2B). Hence the BX3 catalysed 3-hydroxylation of ION is less efficient than endogenous enzymes metabolising ION to yield 5HIONG (see below). The results indicate that in Arabidopsis

Table 2
Metabolisation of BX intermediates by transgenic plants expressing Bx2 to Bx5 and ZmPor2 (Cluster+). (A) In vitro assay applying the individual substrates to isolated microsomes. The transgenic *ZmPor2* plant was used as control. (B) Application of the indicated substrates to cut rosette leaves. Col-0 was used as control. Analysis was by HPLC-UV. n.d. not detectable.

A

Genotype	Substrates			
	Indole	ION	HION	HBOA
Cluster+	ION	HION HBOA	HBOA DIBOA	DIBOA
control	n.d.	n.d.	n.d.	n.d.

B

Genotype	Substrates			
	Indole	ION	HION	HBOA
Cluster+	TRP	5HIONG	HBOA DIBOA GDIBOA	HBOA-Glc HBOA-diGlc GDIBOA
control	TRP	5HIONG	n.d.	HBOA-Glc

Table 3
Metabolite profiles of transgenic Arabidopsis and maize lines. Rosette leaves of 28 dag plants or 4 dag seedlings were used respectively. Absolute quantification of 5HIONG is not possible. The ratio 5HIONG/ION was calculated based on the respective peak area (HPLC-UV analysis). *LC-MS-TOF analysis, **background values. Maize seedling shoots 4 days after imbibition were analysed.

Genotype	TRP [μmol/g DW]	ION [μmol/g DW]	GDIBOA [nmol/g DW]	5HIONG [peak area]	5HIONG/ION ratio	SA [ng/g FW]
Col-0	1.34 ± 0.28	0.28 ± 0.19**	n.a.	n.a.	n.a.	392 ± 217
Bx1C+	2.32 ± 0.22	2.1 ± 0.75	3.7 ± 0.7 *	2.3 ± 0.2	6.2 ± 2.1	124 ± 17
Bx1Bx2C+	1.82 ± 0.26	66.5 ± 9.6	11 ± 2.9 *	58.5 ± 7.5	4.7 ± 0.07	2416 ± 347
Bx1Bx3C+	0.37 ± 0.02	0.89 ± 0.35	42.7 ± 8.8 *	15.2 ± 1.3	7.2 ± 0.75	92 ± 4.7
Bx1Bx2Bx3C+	0.31 ± 0.04	4.35 ± 0.95	194 ± 8.5 *	2.2 ± 0.9	10.5 ± 2.5	52 ± 16.6
Bx1	1.91 ± 0.07	n.a.	n.a.	n.a.	n.a.	n.a.
Bx1Bx2	2.35 ± 1	52.7 ± 13	n.a.	57.6 ± 14	5.8 ± 0.8	1123 ± 99
Bx1Bx2Bx3	0.57 ± 0.1	0.52 ± 0.12	n.a.	1 ± 0.4	10 ± 2.3	64 ± 6
B73 wt	6.6 ± 1.3	0.4**	n.a.	0.79 ± 0.66**	5.2 ± 1.6	20.8 ± 5.1
B73 bx1	10.8 ± 1.2	0.35**	n.a.	0.24 ± 0.14**	6 ± 6.4	n.a.
B73 bx3	11.7 ± 2.2	24	n.a.	2.3 ± 0.5	0.3 ± 0.1	15.1 ± 8.2

channelling of pathway intermediates is scarce or not existing. Enzymes that readily modify the novel compounds, e.g. glycosyltransferases, are available and the resulting modification generates a sink that interferes with the flow of the BX pathway.

The most prominent hitherto unknown compound was detected in the feeding of ION to Col-0 and appeared similarly in the transgenics harbouring *Bx1* and *Bx2* in different combinations (Table 3, 5HIONG). In Bx1C+ the inferred concentration of the compound exceeds GDIBOA by a factor of thousand. For the isolation and characterisation of the metabolite Bx1Bx2 transgenics were used. The metabolite is characterised by a positively charged ion with the *m/z* 312. For structure elucidation the extract was fractionated by solid-phase extraction (SPE) and reversed phase chromatography on a C18 column. Collected fractions were analysed by UPLC-ESI-UV-TOF MS and the fractions containing the target compound were chromatographically extracted on a preparative HPLC column (see 4.12). The purified compound was subjected to NMR analysis and identified as indoline-2-one-5-*β*-D-glucopyranoside (5HIONG, Fig. 2). Hence, ION is hydroxylated and glucosylated by endogenous Arabidopsis enzymes and the product of the conversion is abundant (Table 2). In contrast to DIBOA biosynthesis (Fig. 1), the initial hydroxylation of ION is at position C5 of the aromatic ring (Fig. 2). Across all genotypes of transgenics the relative amount of 5HIONG exceeds ION in rosette leaves (Table 3), in young seedlings (7 dag) both indolinones have similar levels, and at senescence 5HIONG is the only indolinone detected (Supplemental Figure S4).

To get further insight into bottlenecks limiting BX biosynthesis in Arabidopsis, the individual substrates of pathway enzymes were applied to Bx1C + plants and the increase in GDIBOA relative to the buffer control was determined (Fig. 3A). Highest gains of the BX were reached with supplementation of HION and HBOA, hence the critical steps are located upstream of HION biosynthesis. Since the constraint is not overcome with externally supplied ION, BX3 catalysis is a suspected bottleneck in the sequence of reactions. The special importance of efficient ION C3-hydroxylation was validated in a complementary experiment. Crosses of Bx1C+ with individual *p35S* constructs of the P450s were performed and thereby the transcript levels for single genes were raised up to five-fold (Supplemental Figure S2B). Application of the immediate substrate to the respective overexpressors increased the GDIBOA production in the case of *Bx3* to more than six-fold (Fig. 3C) and twofold for *Bx5* (Fig. 3E) compared to the respective substrate application in Bx1C+ (Fig. 3A). No or minor effect was detected for the other genes.

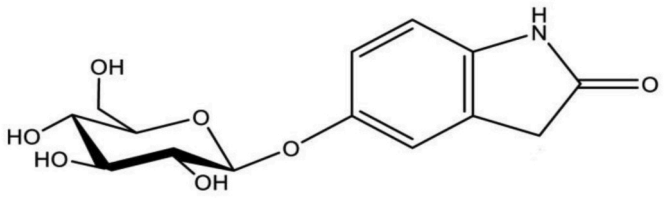

Fig. 2. Chemical structure of indoline-2-one-5-β-D-glucopyranoside (5HIONG).

Plants overexpressing *Bx3* in the Bx1C + background had increased GDIBOA levels in indole feeding (Fig. 3C). Hence BX1 and BX2 enzyme activity might contribute to the efficiency of biosynthesis collectively with BX3. We generated the series Bx1Bx2C+, Bx1Bx3C+ and Bx1Bx2Bx3C + based on an initial cross of Bx1Bx2Bx3 and Cluster+ (Table 1). In accord with the previous results, the highest relative increase is supported by elevation of *Bx3* expression, but *Bx2* contributes to further GDIBOA enrichment and the final concentration reached in transgenic Arabidopsis is 194 nmol/g DW (Table 3).

2.3. TRP and BX biosynthesis are in competition

BX1 delivers free indole, which is also the substrate of the tryptophan synthase beta-subunit (TSB, Fig. 1). Hence competition of the two pathways for the shared substrate might cause a limitation of BX biosynthesis. We detected a significant increase of free TRP in several *Bx1* expressing transgenics, namely BX1, Bx1C+ and Bx1Bx2C+ (Table 3). The increase in concentration of at least 0.48 μmol/g DW is considerable compared to the highest concentrations reached for GDIBOA. However, all transgenics with elevated BX3 enzyme activity (Bx1Bx2Bx3, Bx1Bx3C+, Bx1Bx2Bx3C+) display a reduction of free TRP, irrespective of GDIBOA biosynthesis. Hence, productive establishment of the early part of the pathway increases the flux of indole into BX biosynthesis may be at the expense of TRP. The same tendency is found in maize. Mutants of the genes *Bx1* and *Bx3*, both impaired in BX biosynthesis have an about 50% increase in free TRP concentration (Table 3). Taken together primary and specialised metabolism are in competition and the flux into BX biosynthesis is dependent on BX3 activity.

In contrast to TRP biosynthesis, no impact on the total amount of glucosinolates was detected when the branch of BX biosynthesis is introduced in Arabidopsis (Supplemental Figure S5A). However, the ratio between I3G (indolyl-3-methyl glucosinolate) and 4MI3G (4-methoxyindolyl-3-methyl glucosinolate) is significantly altered indicating, that the plants are facing metabolic stress (Supplemental Figure S5B).

2.4. Metabolic stress induced by expression of BX biosynthesis

Intermediates of BX biosynthesis are recognised by the host and modified. For the most prominent metabolite ION we examined whether metabolisation is specific for Arabidopsis or a general feature in the plant kingdom. We subjected a diverse panel of plant species to feeding with ION (1 mM, Table 4). All plants accumulated ION upon feeding for 8 h (endogenous concentration in leaves, mean value of all plant species 760 ± 21 μmol/g FW) in an amount exceeding the level in unfed

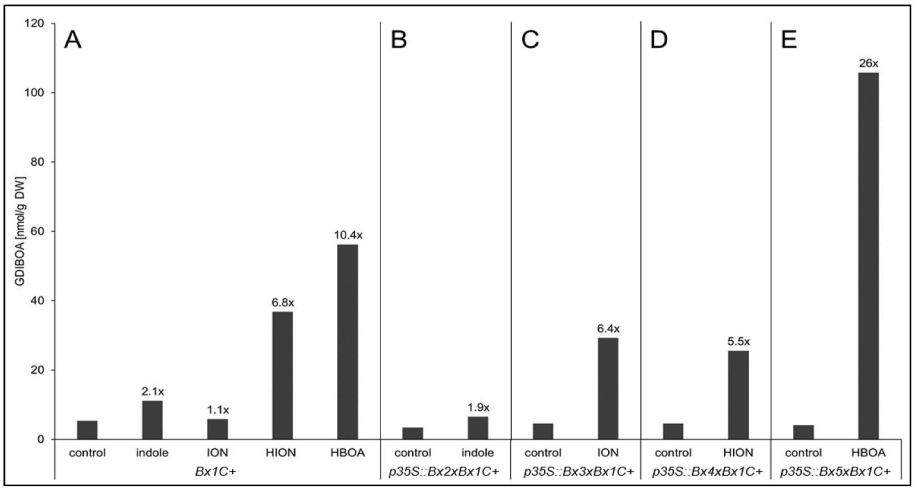

Fig. 3. GDIBOA level in transgenics. (A) Effect of exogenously applied substrates on GDIBOA yield. Feeding of the substrates HION and HBOA led to a substantial increase in GDIBOA concentration in Bx1C + plants compared to the buffer control. (B) To (E) Transcript levels of individual *Bx* genes encoding P450 enzymes were increased by introduction of *p35S* constructs into the basic GDIBOA producing line Bx1C+. (B) *Bx2*, (C) *Bx3*, (D) *Bx4*, (E) *Bx5*. For *Bx2* and *Bx4* overexpression had minor effect on GDIBOA yield when the respective substrate was applied exogenously. In contrast, more than 6-fold (compare A, D) and 2-fold (compare A, E) increase was detected for *Bx3* and *Bx5* in the analogous feeding.

transgenic Arabidopsis (Table 3). Characteristic 5HIONG HPLC peaks were detected in the analysis across the panel. However different plant species metabolised ION at various rates (Table 4). The Brassicaceae species displayed the highest conversion rate (up to 5HIONG/ION rate of 0.125) and exceeding the rate of Poaceae family members (<0.008) by a factor of 26. While no intermediates of the pathway are detected in wild type maize, the *bx3* mutant accumulates ION in the same range as respective transgenic lines, e.g. Bx1Bx2 (Table 3), but a signal of the putative 5HIONG metabolite is less prominent resulting in a significant difference in the 5HIONG/ION ratio in maize and Arabidopsis. The feeding and mutant data indicate that by trend the grasses metabolise ION to a lesser extent compared to dicots.

The supposed steps in 5HIONG biosynthesis are hydroxylation followed by glucosylation. In plants, P450 enzymes (Chapple, 1998) and 2-oxoglutarate dependent dioxygenases (ODDs; de Carolis and de Luca, 1994) predominantly catalyse hydroxylation. To get a hint whether these enzyme classes are employed in ION metabolism, we applied the P450 specific inhibitor 1-aminobenzotriazole (ABT; Kim et al., 2004) or the ODD inhibitor prohexadione (PHD; Rademacher et al., 1992) together with ION to detached rosette leaves of Col-0. A significant reduction of 5HIONG biosynthesis was found in presence of ABT (Fig. 4A). We made the analogous analysis with additional plants, *Pisum sativum* of the order Fabales of the rosids clade (eurosid II), *Nicotiana benthamiana* of the order Solanales in the clade asterids and *Hordeum vulgare* as a representative of non-BX containing monocots of the order Poales (Fig. 4B, C, D). All tested plants accumulated a similar amount of ION and the biosynthesis of 5HIONG was greatly reduced by ABT in all cases demonstrating that employment of P450s is not restricted to Arabidopsis. No significant reduction was found in any application of PHD.

In Arabidopsis P450s are essential for the biosynthesis of GLS and camalexin. Since both are related to the TRP biosynthetic network (Fig. 1) we hypothesised that these monooxygenases might catalyse the C5 hydroxylation of ION. A total of 15 known Arabidopsis P450 enzymes (Supplemental Table S2) most of them involved in indolic glucosinolate or camalexin biosynthesis were analysed by screening of available mutants for reduced 5HIONG production in feeding experiments. However, none of these candidates showed a significant change of the 5HIONG/ION ratio. Taken together, these findings show that ION is probably recognised by plants as an unspecific metabolite and generally hydroxylated at the position C5 by P450s prior to glycosylation. Whether the enzymes have ION hydroxylating activity due to overlap with

Table 4
Metabolisation of ION in different plant species. Ratio of indolinones after feeding. Representatives of the Lamiaceae and Ranunculaceae were included since DIBOA glucoside is found in single species of these families. Likewise, *Sorghum bicolor, Setaria italica*, *Avena sativa*, *Hordeum vulgare* and *H. spontaneum* (Hordeum sp.) representing non-benzoxazinoid producers in the grasses family were analysed (Grün et al., 2005). The low amount of the glycoside in the feeding assay can be attributed to the high level absorbed and the short-time exposure to the substrate, Supplementary data.

Species	Family	Ratio [5HIONG/ION]
Arabidopsis thaliana	Brassicaceae	0.077
Eutrema salsuginea		0.030
Brassica oleracea		0.125
Pisum sativum	Fabaceae	0.010
Lotus japonicus		0.009
Nicotiana benthamiana	Solanaceae	0.009
Ocimum basilicum	Lamiaceae	0.008
Consolida ambigua	Ranunculaceae	0.004
Consolida ajacis		0.007
Delphinium grandiflorum		0.003
Allium porrum	Amaryllidaceae	0.047
Avena sativa	Poaceae	0.002
Setaria italica		0.002
Sorghum bicolor		0.001
Hordeum sp.		0.008

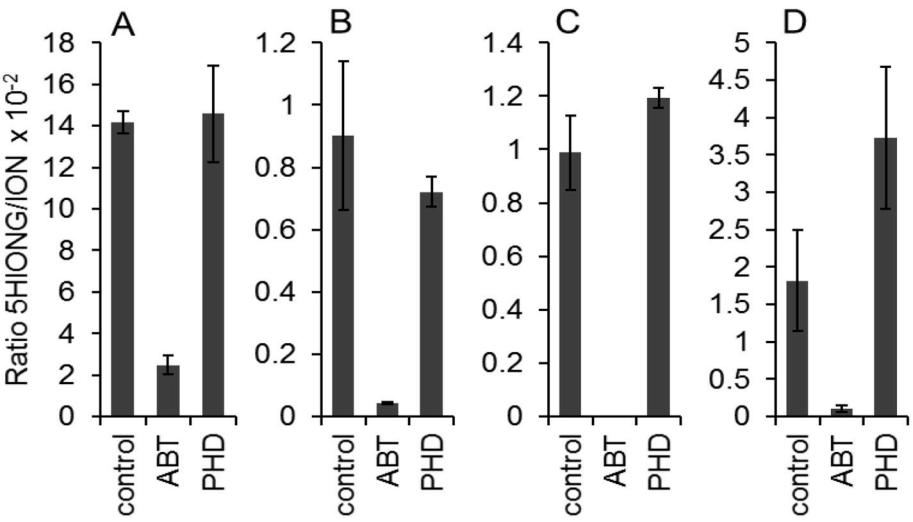

Fig. 4. ION metabolisation in the presence of inhibitors. The analysis was performed with plant species of unrelated families. (A) Arabidopsis Col-0. (B) *Nicotiana benthamiana*. (C) *Pisum sativum*. (D) *Hordeum vulgare*. The plants were fed with ION (1 mM) and ION together with specific inhibitors of P450s (ABT, 0.5 mM) and ODDs (PHD, 0.1%). The ratio of 5HIONG to ION was calculated from the peak areas in HPLC analyses. The ION level detected across the control plants was similar (760 ± 21 μmol/g FW). The mean and the standard deviation of three replicates are given. ABT: 1-aminobenzotriazole, PHD: prohexadione, MES: Buffer control.

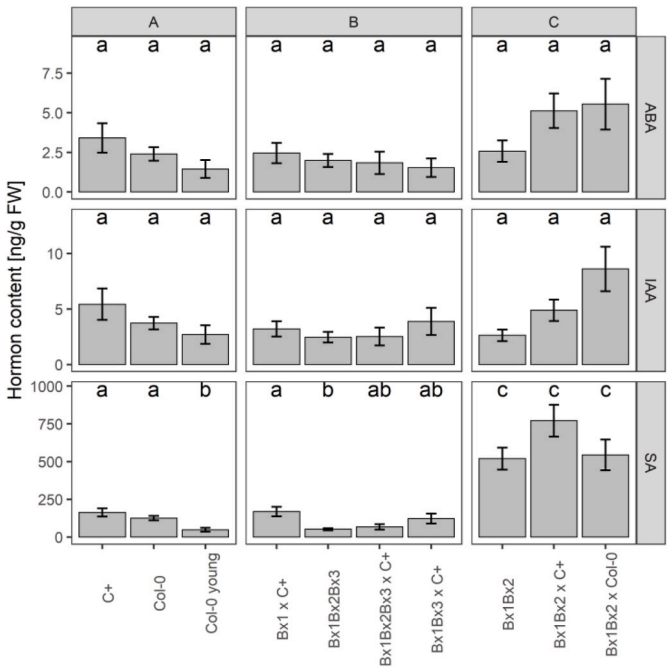

Fig. 5. Hormone content in the transgenics grouped by intrinsic indolinone concentration (Table 3). Control plants containing no ION (A) and plants expressing parts of the BX pathway with low amount of ION (B) do not differ significantly in their hormone levels. Genotypes with high intrinsic ION levels (C) express a significant accumulation of salicylic acid while ABA and IAA levels are not consistently higher. Statistics were as described in 4.15. Different letters denote significant differences according to Tukey's HSD ($P < 0.05$).

substrates of intrinsic pathways or have limited substrate specificity is not yet elucidated.

2.5. The indolinone chemotype has impact on hormone homeostasis

Biosynthesis of the intermediate ION and the derived 5HIONG reached considerable concentrations in Arabidopsis exceeding in e.g. Bx1Bx2 the level of TRP by far (Table 3). Hence, the two indolinones represent a significant metabolic sink. In addition, the metabolites have biological activity as depicted by dose dependent reduction of root growth when applied exogenously (Supplemental S6). Transgenic lines that contained significant levels of the phytotoxic indolinones (>50 μmol/g DW; Bx1Bx2C+, Bx1Bx2; Table 3) displayed a change in phytohormone homeostasis compared to lines with lesser concentrations (<4 μmol/g DW; Bx1C+, Bx1Bx3C+, Bx1Bx2Bx3C+, Bx1Bx2Bx3, Table 3) and the control Col-0. Auxin levels were not consistently changed in correlation with ION/5HIONG (Fig. 5) although auxin and indolinones are directly connected in the metabolic network (Fig. 1). Furthermore, the auxin distribution pattern in the embryo was not influenced by indolinones in transgenics (Supplemental Figure S7). Hence, the sink effect of the indolinones does not seem to have greater relevance. Both, abscisic acid (ABA) and salicylic acid (SA) are increased in the "high" indolinone plants (Fig. 5). The ABA content featured some variation in repeated analysis and increased in the presence of indolinones only by trend. The impact of indolinones on SA was significant, therefore, SA connected features were analysed in detail.

To distinguish immediate and SA mediated effects, we introduced the SA hydroxylase, *NahG,* by crossing to Bx1Bx2 plants. The resulting progeny has a high concentration of indolinones and a SA level at the detection limit (Supplemental Figure S8). Analysis of the *NahG* expressing transgenics at transcript level revealed that the abundance of the pivotal genes in biosynthesis and catabolism ICS1, and S3H was not correlated with the presence of indolinones. Likewise, regulatory genes were not influenced and both the transcript level of the marker genes for SA mediated defence response *PR-1* (*PATHOGENESIS-RELATED 1*) and for the interconnected NHP1 dependent defence, *FMO1* (*FLAVIN-CONTAINING MONOOXYGENASE 1*; Vlot et al., 2009), were not increased by indolinones in NahG plants (Supplemental Figure S9). The connection between indolinones and adjustment of SA levels is rather indirect and might be caused by SA regulatory circuits.

Beside the correlation between constitutive exposure to indolinones present in transgenics and increased SA levels, we found that by trend also exogenous application of ION to cut leaves was a trigger for raised SA concentration although the main impact in this experiment was wounding of the plants (Supplemental Figure S10). Reversely, with the reduction of SA in *NahG* expressing plants a decrease in the metabolisation of ION is detected in transgenics (Bx1Bx2 *vs. BX1Bx2 x NahG*) and in exogenous application of ION (Col-0 vs. *NahG* plants). In both cases the ratio of 5HIONG/ION is significantly reduced in the respective *NahG* genotypes (Supplemental Figure S11). The potentially phytotoxic metabolite ION induces a shift in SA concentration and its modification is increased in the presence of SA.

2.6. Indolinones have an impact on plant morphology

Transgenic plants expressing *Bx*-genes show morphological differences in correlation with the presence of indolinones (Fig. 6,

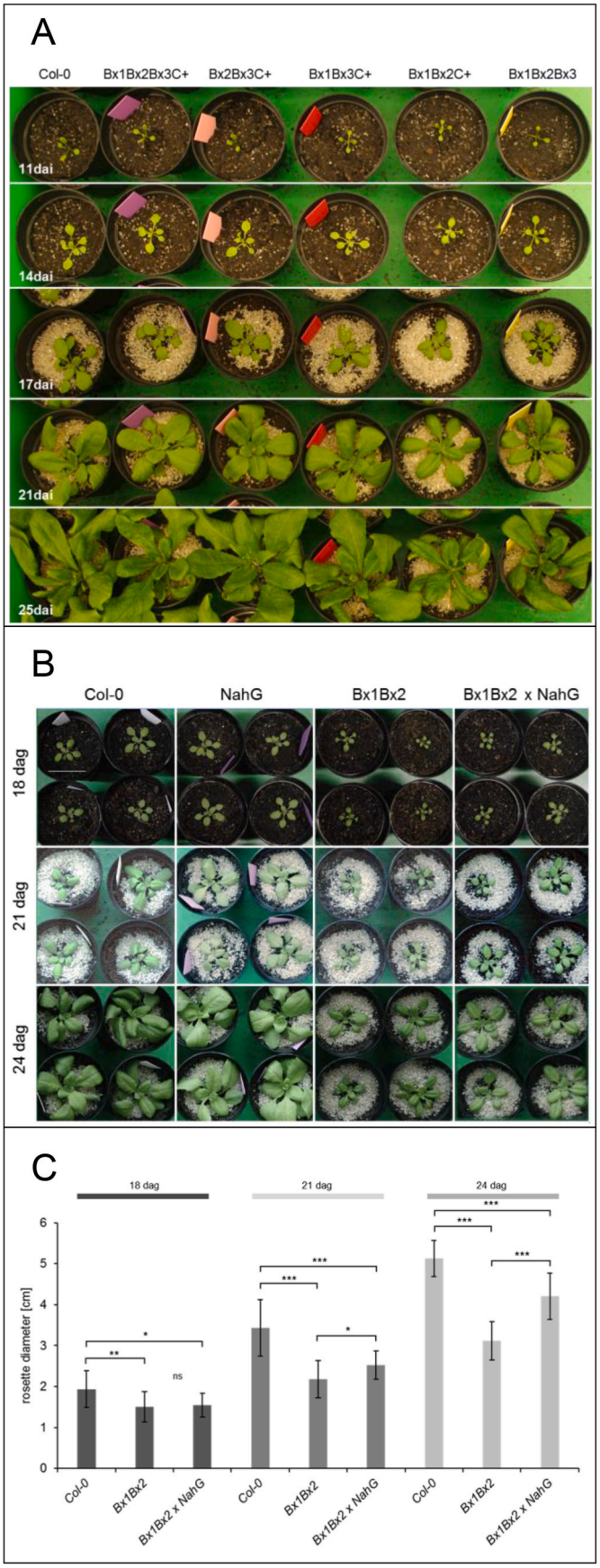

Fig. 6. Phenotype of transgenics. (A) Representative plants of the lines Col-0, Bx1Bx2Bx3Cluster+, Bx2Bx3Cluster+, Bx1Bx3Cluster+, Bx1Bx2Cluster+ and Bx1Bx2Bx3, 11 to 25 dag are displayed. Transgenics containing GDIBOA and minor concentrations of indolinones (Bx1Bx2Bx3C+, Bx1Bx3C+; Table 3) have wild type phenotype. The line Bx1Bx2C+ with high ION/5HIONG content is filigree. Bx1Bx2Bx3 resembles Col-0. (B) Four representative plants of the lines Col-0, NahG, Bx1Bx2, *Bx1Bx2 x NahG* from left to right, at 18, 21, 24 days after germination (from top to bottom). (C) Rosette diameter of Col-0, Bx1Bx2 and *Bx1Bx2 x NahG* plants from the left to the right, 18, 21 and 24 days after germination. Mean and standard deviation for 14 plants each are given. Asterisks indicate * $p < 0.05$, ** $p < 0.01$, *** $p < 0.001$ using Student's *t*-test. ns: not significant, dag: days after germination.

(caption on next column)

Supplemental Figure S12, Table 3). The most extreme phenotype is displayed by *p35S::Bx1 p35S::Bx2* plants that are dwarfed and both male and female sterile (Supplemental Figure S12 B). Bx1Bx2 are fertile, have prolonged time to flowering, retarded growth and are filigree (Supplemental Figure S12A). The phenotype is reverted in all transgenics that have reduced ION concentration, e.g. by enhanced expression of *Bx3*, irrespective of the concentration of GDIBOA (Bx1Bx2Bx3Cluster+, Fig. 6 A, Bx1Bx2Bx3, Supplemental Figure S12). Although SA was first recognised as a hormone involved in basal defence against pathogens (Vlot et al., 2009), recent data imply that the phytohormone additionally plays a role in plant responses to development (Lee et al., 2010; Rajjou et al., 2006), vegetative growth and senescence (Šašek et al., 2014; Scott et al., 2004; Vogelmann et al., 2012). The altered morphologies associated with high indolinone levels might thus be caused indirectly by disturbed SA homeostasis as described for several genotypes affecting SA levels and SA signalling (Pluhařová et al., 2019; Šašek et al., 2014). When indolinones were analysed separated from SA accumulation in *Bx1Bx2 x NahG* the plants still showed significantly reduced growth compared to Col-0 (Fig. 6 B, C). The morphological phenotype was enhanced in the presence of SA. Bx1Bx2 plants have smaller rosettes and narrower leaves compared to the *Bx1Bx2 x NahG* counterparts. Hence, indolinones influence plant morphology partially through their effect on SA homeostasis but there is also a SA independent indolinone effect.

3. Discussion

3.1. Transgenic Arabidopsis synthesises GDIBOA

With the transfer of six *Bx*-genes and the maize P450-reductase gene we could establish BX biosynthesis in Arabidopsis. The maximum yield in rosette leaves was about 0.2 μmol/g DW, hence 50-fold below the concentration required for the control of pathogens and insects. The effective concentration was determined to be higher than 10 μmol/g DW (deduced from FW data of 1 μmol/g; Campos et al., 1989; Long et al., 1975) and the concentration of BXs in original producer plants is even higher. Values of above 30 μmol/g FW are reached in the dicot *Consolida orientalis*, and around 20 μmol/g FW in maize (Schullehner et al., 2008). The high concentration of BXs is not an exceptional feature with respect to defence metabolites, e.g. GLS in *Brassica oleracea* and CG in *Sorghum bicolor* are present at levels of 3–18 μmol/g FW (Halkier and Møller, 1989; Møldrup et al., 2012; Staley et al., 2009). Adequate biosynthesis of the compounds might require significant resources and constraints of the plant's metabolism might limit the efficiency of transgenic pathway expression. However, in the case of CG in Arabidopsis and GLS in *N. benthamiana* the concentrations achieved in the "host " transgenic plants were similar to the source plant's level (Møldrup et al., 2012; Petersen et al., 2018; Tattersall et al., 2001). A hint that metabolism is challenged in the transgenic approaches is given by the finding that additional supply of sulphur and streamlining of sulphur metabolism supported intrinsic GLS biosynthesis in brassicaceous plants as well as in transgenics (Møldrup et al., 2011; Petersen et al., 2018). CG and GLS biosynthesis both are extensions of primary metabolism and use an

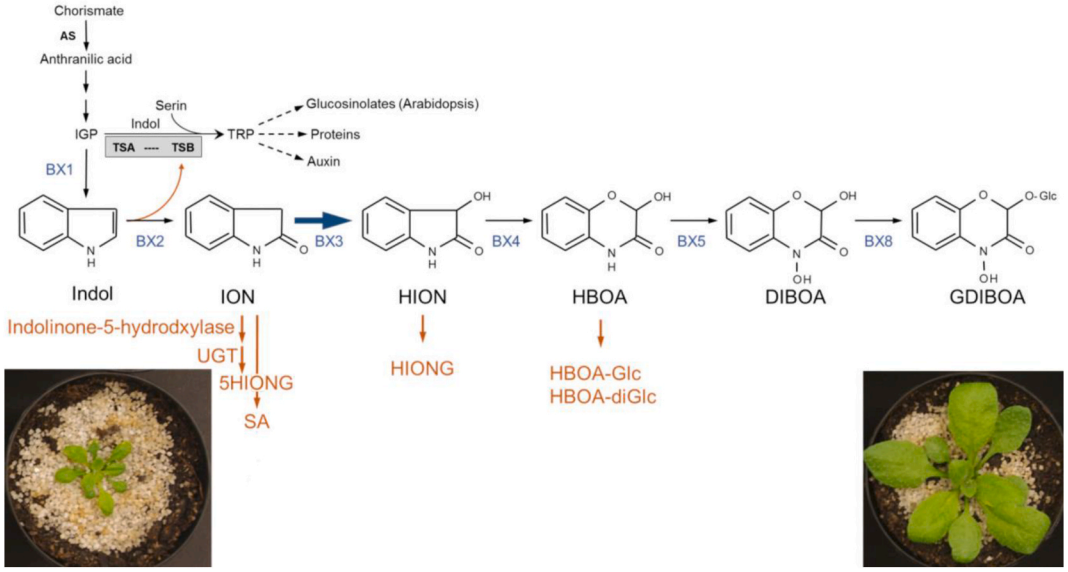

Fig. 7. Metabolic changes and consequences of BX expression in Arabidopsis. Reaction steps, compounds and enzymes that are specifically detected in transgenic Arabidopsis are marked in orange. Critical for BX biosynthesis is C3-hydroxylation by BX3. BX3 is in competition with an intrinsic C5-hydroxylase that opens a new biosynthesis branch leading to enrichment of 5HIONG. ION and 5HIONG accumulation is connected with increase of SA. High levels of the indolinones result in morphological changes that are increased in the presence of SA. GDIBOA containing plants have wild type morphology. Auxin and total GLS levels are not significantly changed. (For interpretation of the references to color in this figure legend, the reader is referred to the Web version of this article.)

amino acid to start the pathway. In contrast, BX and TRP biosynthesis branch and the flux in host plants maybe in favour of the primary metabolite (Fig. 7). . In the transgenics free TRP concentration increased with the expression of BX1 (that delivers indole) when concurrently BX biosynthesis was incomplete or at low level (i.e. genotypes Bx1Bx2, Bx1C+, Bx1Bx2C+, Table 3). But the concentration of TRP was reduced in all genotypes with increased BX3 enzyme activity (i.e. lines Bx1Bx2Bx3, Bx1Bx3C+, Bx1Bx2Bx3C+) showing that BX biosynthesis competes with the TRP biosynthesis. In maize TRP concentration is influenced by BX biosynthesis as well with increased levels in BX mutants (Table 3). Recent data show specific interaction between the monocot-specific isoforms of the indole-3-glycerolphosphate synthase enzymes (IGPS 1, IGPS3) present in maize (Richter et al., 2021) with the indol-3-glycerol phosphate lyases BX1 and IGL. Interaction with TSA is mainly by IGPS2 that is considered as the ortholog to the single enzyme encoded in Arabidopsis (Richter et al., 2021). The expression pattern of IGPS1, IGPS3 implies a function rather in defence than in primary metabolism. The interdependence of the two pathways in Arabidopsis might be explained by the presence of the single IGPS. In maize seedlings the competition between the IGPS isoforms might influence the relative levels of TRP and BXs. Extreme concentrations in BX producing plants may therefore be restricted through metabolic limitation to developmental stages (e.g. seedlings in the grasses) and organs (e.g. flowers of *C. orientalis*; Schullehner et al., 2008), but there is no exclusion of a specific organ indicating a general tolerance to the compound. Restriction of BX biosynthesis to certain developmental stages or organs might balance between defence and development in the particular plant. In the transgenic approach narrowing of pathway expression spatially or temporally might allow an enrichment of BXs.

3.2. Presence of intermediates and consequences

A crucial difference between transgenics and source plants is the presence of intermediates and metabolites thereof, which are not described in maize and other BX plants (Fig. 7). Loss of intermediates can be reduced by channelling of substrates along the biosynthetic pathway mediated by enzyme interaction. Transient multi-protein complexes of sequential enzymes are named metabolons (Laursen et al., 2015; Zhang and Fernie, 2021). The overall pathway efficiency in metabolons is increased by local enrichment of substrates and possibly by allosteric interactions that influence enzymatic properties. Metabolons are suggested to exist especially for secondary metabolic pathways (Zhang and Fernie, 2021 and citations therein) since an additional characteristic feature is scarce leakage of potentially toxic intermediates (Laursen et al., 2015). For dhurrin biosynthesis the metabolon is established and especially channelling and allosteric activation is proven. It has been shown that the interaction of P450s and the respective pathway UGT are required for dhurrin biosynthesis. The same enzyme classes are integral parts of BX biosynthesis. However, no evidence for the formation of a metabolon for BX biosynthesis in the grasses or BX producing dicots is available beside the lack of intermediates. In the transgenics, all presumed constituents of a BX metabolon, including the maize POR that might serve as an ER anchored nucleation structure for the P450s (Jørgensen et al., 2005; Winkel, 2004), are expressed. We found that the enhancement of *Bx3* expression was the key for the raised GDIBOA biosynthesis in Arabidopsis (Fig. 3, Table 3, Fig. 7). BX3 was shown to be in competition with intrinsic ION 5-O-hydroxylating enzyme(s) (Figs. 4 and 7) and the loss of the intermediate is a substantial obstacle in the flow of the pathway. Since endogenous P450s play a major role for this alternative ION hydroxylation in Arabidopsis enhanced BX3 expression might increase productive association with PORs, maybe at the expense of accommodating of the intrinsic enzymes. Whether the effect of stoichiometry between BX3 and intrinsic P450s matters in this respect or high BX3 levels might allow the initiation of a metabolon, namely a channelling of the intermediate from BX2 to BX3, is unknown.

3.3. Indolinones are biological active and generally subject to modification

ION, the first intermediate of BX biosynthesis that is not a common metabolite in plants has phytotoxic properties as demonstrated by reduction of root growth (Supplemental Figure S6) at concentrations lower than present in transgenic plants (Table 3). A similar effect was described for 3-acetonyl-3-hydroxyindolin-2-one in *N. benthamiana* (Li et al., 2008). Outside the plant kingdom the indolinone 5HION was

described as excretion product of animal metabolism a long time ago (Beckett and Morton, 1966) and might function in rhythmic adjustments in the brain (Crumeyrolle-Arias et al., 2008). 5HION interferes with protein kinases, which might contribute to antiproliferative and pro-apoptotic effects of the compound (Cane et al., 2000). Although free indole is not prevalent in plants due to the channelling in the tryptophan synthase complex and the lack of tryptophanases, it is emitted by some plants during flower development or induced by herbivore infestation as part of cocktails of volatile compounds (Frey et al., 2000). Similarly, indole functionalisation by hydroxylation is basal in the biosynthesis of the pigments indigo, indican and isatin. It was proposed (Maier et al., 1990) and recently shown for *Polygonum tinctorium* that free indole is substrate in the biosynthesis. In this case hydroxylation is catalysed by a flavin-containing monooxygenase (FMO, Inoue et al., 2021). Hence plants might encounter bioactive indolinones. ION seems to activate a default route of metabolisation in plants consisting in hydroxylation by P450s as first step and consecutive glycosylation of 5HION (Fig. 2, Table 4). Based on structural similarity of the substrate Arabidopsis P450s involved in GLS and camalexin biosynthesis were candidate hydroxylases for 5-hydroxylation of ION, but the enzymes investigated by analysis of mutants had no significant impact on ION metabolisation. Given that ION hydroxylation was evident in plants across the kingdom there could be in analogy to animal systems a reservoir of unspecific oxygenases employed for detoxification of xenobiotics in parallel to pathway-specific P450s. Glycosylation is known to be a general modification of alien compounds, e.g. xenobiotics and allelochemicals (Jones and Vogt, 2001; Schulz et al., 2016) and was also detected for the intermediates HION and HBOA. However, the efficient metabolisation of ION and massive accumulation of 5HIONG in Arabidopsis did not exclude a major impact on plant morphology (Fig. 6, Supplemental Figure S12, Fig. 7). Since 5HIONG is not commercially available and application of ION goes together with 5HIONG biosynthesis in plants the toxic effect of the compounds could not be separated. 5HIONG however seems to be a stable storage compound (Supplemental Figure S4).

3.4. Chemotype and chemotype variation

Expression of *Bx* genes in Arabidopsis was expected to interfere with auxin and indolic GLS homeostasis via the TRP network (Fig. 7). We found pronounced alterations of the chemotype correlated with the biosynthesis of ION. However, neither auxin nor total glucosinolate concentration was significantly influenced by the substantial flow into the transgenically established pathway. Within the indolic GLS a significant shift from I3G to 4MI3G was observed in transgenics (Supplemental Figure S5). 4MI3G is a signature compound for stress conditions (Yang et al., 2020), hence not limitation of substrates due to the introduction of the BX branch into the network but rather the toxicity of the intermediate ION disturbs the metabolic homeostasis. A significant correlation was detected between ION and SA in Arabidopsis. Increase of SA, as a reaction to changes in specialised metabolite profile seems to be common in Arabidopsis. Elevated SA concentration was also recognised connected with the appearance of novel GLS after transgenic expression of P450s that catalyse reactions in CG biosynthesis (Brader et al., 2006). For ION we found a mutual interaction: SA levels increased with ION levels, and 5HIONG biosynthesis is elevated in the presence of SA (Supplemental Figure S11, Fig. 7). The extent of ION metabolisation varies greatly between the analysed representatives of plant families with the Brassicaceae having the highest ratio and lowest ratios detected in the Poaceae (Table 4). This might reflect a basic tolerance to ION in the Poaceae family that characteristically synthesises BXs. In agreement with this finding, the SA level in the indolinone-containing *bx3* mutant is not significantly increased (Table 3). Hence ION causes metabolic stress in Arabidopsis but is tolerated in maize. Within the dicots the Brassicaceae proved to be highly sensitive to the metabolites and other families, e.g. Solanaceae might allow higher concentrations of BX in transgenic approaches.

3.5. Direct and indirect effects of ION on the phenotype of transgenics

In the presence of GDIBOA the transgenic lines had wild type phenotype but lines with high concentration of indolinones (ION or 5HIONG, Table 3) were filigree and retarded in bolting and senescence (Supplemental Figure S12, Fig. 7). Since these transgenics had elevated levels of SA at the same time (Fig. 5) the morphological aberrations might be caused by the disturbed SA homeostasis as described (Šašek et al., 2014). Analysis of SA impaired NahG transgenics proved that the presence of indolinones influences the morphology in Arabidopsis independent of SA (Fig. 6B and C). Again a difference to maize is detected since *bx3* mutants do not differ from wild type in development and especially the seedlings that possess high concentration of ION are not distinguishable from wild type counterparts.

3.6. Insight into the evolution from transgenic expression of BX biosynthesis

All intermediates of the pathway seem to be modified in Arabidopsis by glycosylation. A contribution of the UDPG: DI(M)BOA-glucosyltransferase BX8 is questionable since *in vitro* activity towards the intermediates is low or missing (von Rad et al., 2001) and glycosylation is also detected after feeding of Col-0 with the compounds. Intriguingly, in contrast to this immediate glycosylation of intermediates, none of the about 100 members of the UGT family in Arabidopsis is suitable to glycosylate the final reactive BXs DIBOA and DIMBOA (Dick et al., 2012; von Rad et al., 2001). Similar results were found for the glycosylation of intermediates on one hand and the final compound on the other in transgenic CG biosynthesis (Tattersall et al., 2001). The specific UGT of CG biosynthesis is part of the metabolon and ameliorates biosynthesis by influencing enzymatic properties of the individual enzymes (Knudsen et al., 2018; Laursen et al., 2016). The efficiency of the biosynthesis seems to be coupled to the final reaction that stabilises the compound and thereby reduces autotoxicity. This dual function implies that the recruitment of pathway specific UGT genes was an important factor in evolution of plant specialised metabolite biosynthesis. The establishment of defence compound biosynthesis might have been “from the end” as suggested by Horowitz (1945) for biochemical biosyntheses.

With respect to the branch point of the BX pathway data from dicots, Schullehner et al. (2008) demonstrated that the evolutionary recruitment of a paralogue to TSA that delivers free indole was repeated and achievable in different ways with minor changes in the amino acid sequence. Corresponding with the apparent facility to evolve a suitable indole glycerole-phosphat lyase phylogenetic analysis shifted the critical step in pathway evolution to the first P450 in the chain, *Bx2* (Dutartre et al., 2012). The data of BX transgenic plants indicate that it is essential that the ION synthesised by BX2 is readily modified to reduce its phytotoxic potential and to enforce the flux into specialised metabolite biosynthesis. Recruitment of a suitable hydroxylase, BX3, might have been crucial for establishment of BX biosynthesis. Latent insensitivity to indolinones present in the Poaceae might have favoured pathway evolution in grasses or developed in parallel to BX pathway evolution for metabolic adaptation.

4. Conclusion

A motivation for the transfer of BX biosynthesis to Arabidopsis was to evaluate whether the arsenal of chemical defence can be enlarged in crops by expression of an alien specialised metabolite pathway. Data in the literature demonstrate that this strategy can be successful. With our transgenic approach, we generated GDIBOA in Arabidopsis (Fig. 7) however, an effective BX concentration was not achieved. There was no limitation of the flux into the specialised metabolite pathway due to interference with the primary metabolism since the molar concentration of the first characteristic intermediate ION was in the range needed for

herbivore control by BX, however, consecutive catalysis was inefficient. The plants were dwarfed due to expression of BX genes. We found that it was essential to overcome the barrier built by endogenous modification of the first specific intermediate ION through overexpression of *Bx3*. Increasing and balancing the expression level of all six *Bx* genes, maybe in defined organs or in an inducible way might allow to install BXs as defence metabolites by transgenic expression.

5. Experimental

5.1. Standards and reference compounds

Chemicals were obtained from Carl Roth (Karlsruhe, Germany), Merck (Darmstadt, Germany), Honeywell (Seelze, Germany). Salicylic acid-d_4 was obtained from Olchemim (Olomouc, Czech Republic). Benzoxazinoids were gifts from Prof. D. Sicker, University of Leipzig, Germany, or prepared as described by von Rad et al. (2001). HBOA was purchased from Curpys Chemicals (Kiev, Ukraine). H_2O for LC-MS analysis was purified with an AQUA-Lab-B30-Integrity system (AQUA-Lab, Ransbach-Baumbach, Germany) or with a Milli-Q Gradient A10 system (Millipore, Schwalbach, Germany).

5.2. Molecular biology methods

DNA and RNA isolation, cDNA synthesis, cloning, and PCR amplification was with standard methods as described by Schullehner et al. (2008). Quantitative reverse transcriptase PCR (qRT-PCR) was carried out with a Step One Plus instrument (Thermo Fisher Scientific ABI Applied Biosystems, Germany) using a Kappa Sybr Fast ABI Prism Kit (Merck Sigma-Aldrich, Germany). The cytosolic glucose-6-phosphate dehydrogenase gene (*GAP C*) was used for normalization in quantitative PCR. Defined quantities of purified and cloned fragments of the respective genes were used for establishment of calibration curves and consecutive absolute quantification. The codon-adjusted "Cluster" DNA sequence was designed in two pieces and joint by ligation *via* unique restriction sites (Supplemental sequence) into the T-DNA vector Ti-plasmids pGPTV-Bar B. Primers were purchased from Microsynth, Switzerland, and Eurofins Genomics, Germany. The sequences are given in Supplemental Table S3. For the selection of homozygous T-DNA tagged Arabidopsis lines DNA was isolated by grinding leaf material in extraction buffer (200 mM Tris-HCl, pH 8.0, 250 mM NaCl, 25 mM EDTA, 0.5% SDS). After removing the debris by centrifugation, the DNA was precipitated with an equal volume of isopropanol and collected by centrifugation. The DNA pellet was washed with 70% ethanol and dissolved in TE (10 mM Tris, 0.5 mM EDTA, pH 8.0) buffer. Gene specific primers were used in combination with T-DNA border primers to verify integration, and used in pairs to detect the respective wild type bands (Supplemental Table S1). The presence of T-DNA insertions was verified by sequencing of the PCR fragment. Sequencing was accomplished by Eurofins Genomics, Germany. Segregation of *Bx*-genes in Cluster + plants was analysed by PCR using the gene-specific primers and DNA isolated as described.

5.3. . Arabidopsis transformation

Arabidopsis Col-0 was used for floral dip transformation with Agrobacteria strains GV3001 MP90 and GV3001 MP90 RK harbouring the Ti-plasmids pGPTV-Bar B and the Ti-plasmid M001 based vector 4/1 (Frey et al., 1990).

5.4. Plant material

5.4.1. Arabidopsis lines

The standard promoters *pNos* and *p35S* that mediate moderate-low and high constitutive expression were used to drive genes in transgenics. To avoid promoter redundancy, additional suitable were selected based on the profiles in the Arabidopsis eFP browser developmental map (Winter et al., 2007). The criteria were moderate to high gene expression in rosette leaves with simulantious low transcript level in the flower, since previous analysis had shown that fertility was impaired by *Bx*-gene expression (Lenk, 2015). The promoters of the genes *SUPERROOT2* (*Cyp83B1*) gene (*pSUR2*), *Cyp83A1*, *Cyp79B2* and *Cyp71B7,* genes of GLS biosynthesis were chosen. It has been shown recently that genes of aliphatic (Cyp83A1) and indolic (*Cyp71B7, Cyp79B2*, *Cyp83B1)* GLS biosynthesis have distinct but overlapping expression patterns (Nintemann et al., 2018). The maize BX5 enzyme had low enzyme activity in Arabidopsis, and the orthologous *BX5* gene from wheat (Nomura et al., 2005) was more efficient in transgenic Arabidopsis lines and hence used in the following. The four genes were joint in one T-DNA construct (Supplemental Figure S1) and the coding sequence was adjusted to Arabidopsis codon usage (GeneArt life technologies, Thermo Fisher Scientific). The genotypes of *Bx*-gene transgenics are given in Table 1. The *p35S* and *pNOS* constructs drive the unmodified maize cDNAs. The sequences of the *pSUR2* promoter and promoter/terminator sequences of *Cluster* are given in Supplemental text. Primary transgenic lines were selected based on expression rate of the transgenes. All transgenes had steady state mRNA levels at the range or above of the housekeeping gene *GAP C*.

Different genotype combinations were established by crossing of the homozygous plants and the progeny was analysed. Additional lines were kindly provided by Anton Schäffner, Helmholtz Zentrum Munich (homozygous *NahG* expressing Arabidopsis) and Erich Glawischnig, Professorship Microbial Biotechnology TUM Campus Straubing (P450 genes mutants). Additional insertion lines of P450 genes and the fmo1 mutants were ordered from Nottingham Arabidopsis Stock Center NASC (Supplemental Table S2). The seed sources were the Salk Institute Genomic Analysis Laboratory, GABI-Kat (Kleinboelting et al., 2011) and the WiscDsLox T-DNA collection (Woody et al., 2007).

5.4.2. Maize lines

The line B73 was used as wild type reference. The original mutant lines for *Bx1* and *Bx3* (Frey et al., 1997) were crossed with B73 and homozygous mutant lines were selected after at least six cycles of backcrossing and are named B73 bx1 and B73 bx3.

5.4.3. Other plants

Nicotiana benthamiana seeds were kindly provided by the Institute of Genetics LMU Munich, and *Hordeum vulgare* by Günther Schweizer LFL Freising. Caroline Gutjahr, Plant Genetics, TU Munich kindly supplied us with *Lotus japonica* plants. All other seeds were purchased by Templiner Kräutergarten, Templin, Germany, and Dehner Gartencenter, Freising, Germany.

5.5. Plant growth conditions

Maize was germinated at 28 °C in the dark in wet germination paper and harvested after 4–6 days. All other plants were grown in the GroBanks (CLF Plant Climatics, Germany) at a 16 h light (350 μmol m^{-2} s^{-1}, GroLEDs and cLEDs)/8 h dark cycle at 22 and 18 °C respectively. Standard soil CL-T SM (Einheitserde-Werk Gebr. Patzer, Germany) mixed with quartz sand (5:1) was used in round pots (diameter 4.5 cm) for Arabidopsis and in square pots (8.5 × 8.5 cm) for all other plants. Stratification of *Arabidopsis* was for at least 2 days at 8 °C. *Arabidopsis* rosette leaves were harvested directly into liquid nitrogen at around 30 days after germination. To diminish plant to plant variation 5 to 10 leaves from 5 to 20 individuals were combined for metabolite analysis and in feeding experiments. All genotypes were grown side by side.

5.6. Root growth assay

Seeds were shortly washed with 80% ethanol and sterilised by incubation in 1.3% hypochlorite, 0.1% Triton X-100 (Arabidopsis and

H. vulgare) and 0.8% hypochlorite (*N. benthamiana*). After extensive washing with sterile water, the seed was spread on half strength Murashige-Skoog media, 10 g/L sucrose, 0.8% agar plates, *H. vulgare* was germinated on wet germination paper at room temperature in the dark. After emergence of the root Arabidopsis and *N. benthamiana* were transferred to agar plates supplemented with different concentrations of ION and control plates. The plates were incubated vertically in the growth chamber. Root length was determined 7 days (Arabidopsis) and 11 days (*N. benthamiana*) after imbibition. Germinated *H. vulgare* was transferred to germination paper soaked in watery solutions of the different concentrations of ION. Rolls of the paper were placed vertically in containers and supplied with saturating amounts of the respective ION solutions. The containers were covered with plastic bags and incubation was at 22 °C for 3 days.

5.7. Analysis of GFP expression in transgenics

Analysis was as described in Luichtl et al. (2013). Photographs were taken using a ZEISS Axiophot 1 microscope equipped with a Digital Nikon camera (F5SLR) and corresponding software (Nikon Camera Control Pro).

5.8. Plant feeding

Depending on the species, plants of different age were used in feeding experiments. For dicots, fully developed leaves of young plants before flowering were detached whereas monocots were cut 1 cm above ground when their size was around 15 cm in V1–V4 stage. 4 weeks old Arabidopsis plants were used. The substrates indole, ION, HION and HBOA were first solved in methanol and dissolved in 50 mM MES pH5.7 1:1000 to a final concentration of 2 mM, 1 mM, 0.5 mM and 0.3 mM respectively. In inhibition assays either 500 μM 1-aminobenzotriazole or 0.1% prohexadione were used for the inhibition of monooxygenases or ODDs respectively. Mock solutions contained 1‰ methanol. Detached leaves or plantlets were incubated in the feeding solution under light for 8 h in the growth chamber. The substrate solution was wiped off and the material was frozen in liquid nitrogen.

5.9. Isolation of Arabidopsis microsomes and P450 assay

15 g of rosette leaves of 28 dag Arabidopsis plants were ground in 200 mL extraction buffer (100 mM ascorbic acid, 1 mM EDTA, 100 mM Tris, 20% v/v glycerol, 20% w/v Sucrose, 5 mM Dithiothreitol) with 4.5 g Polyklar AT (Merck) and sea sand. The raw extract was filtered through cloth and centrifuged twice at 15 000 g for 10 min. Microsomes were isolated from the supernatant by centrifugation at 120 000*g* for 40 min and resuspended in 1 mL suspension buffer (50 mM potassium phosphate buffer pH 7.5, 20% v/v Glycerol, 1 mM Dithiothreitol). The integrity of the microsomes was tested by measuring the cytochrome C reductase activity as described by Urban et al. (1990).

The *in vitro* activity of the BX P450 enzymes was tested by incubation of 1 mg total microsomal protein with the respective substrate (2 mM Indole, 1 mM ION, 250 μM HION, 200 μM HBOA) in 100 mM potassium phosphate buffer pH 7.5 and 1 mM NADPH at room temperature. The reaction was stopped after 30 min by addition of 1 vol methanol and precipitated protein was pelleted by centrifugation. 2.5 vol of 100 mM acetic acid were added to the supernatant and the products were extracted three times with 2 vol of ethyl acetate. The solvent was evaporated in a vacuum centrifuge, the remaining products were resolved in methanol and analysed by HPLC.

5.10. Preparation of plant extracts

Rosette leaves of 28 days old plants were analysed. Plant leaves were frozen in liquid nitrogen and freeze dried. Lyophilised material was ground to fine powder. 50 mg of the material was extracted using 500 μL of the ISTD solution containing 0.004 mg/mL 4-Methylumbelliferyl-β-D-glucuronide in methanol and 2 more times using 500 μL pure methanol. The solvent was evaporated in a vacuum centrifuge and the dried material was solved in a final volume of 100 μL methanol for analysis via HPLC or LC-MS.

5.11. HPLC analysis

Reversed phase HPLC analysis was performed on a Dionex Ultimate 3000 system (Thermo Fisher, Waltham, Usa) with a MultoHigh 100-5μ RP18 250 × 4mm column (Göhler HPLC-Analysetechnik, Chemnitz, Germany) at 40 °C. 0.3% formic acid was used as aqueous solvent (A) and methanol as organic solvent (B), the flow rate was 1 mL per minute. The injection volume of extracts was 5 μL. The following gradient profile was used for the detection of GDIBOA in Arabidopsis extracts: 3min. 12% B, 12min 50% B, 17min. 50% B, 18min. 100% B, 20min. 100% B, 21min. 12% B, 22min. 12% B. For the analysis o 5HIONG and ION content in plant extracts a separate program was used: 4min. 10% B, 5min. 12% B, 14min. 50% B, 19min. 50% B, 20min. 100% B, 22min. 100%B, 23min. 10% B, 24min. 10% B. Separation of HBOA and DIBOA was possible with an isocratic program using 10% acetic acid as the aqueous solvent which was applied to the column at 100% during 40 min followed by 2 min of pure water, 2 min of methanol and 2 min water before equilibration back to 100% solvent A. The Dionex Chromeleon 6.80 software was used for analysis and quantification. Metabolites were quantified using a dilution series of the respective substance of at least 8 steps. The peak area was plotted against the amount of substance and the regression was calculated.

5.12. Analysis by LC-ESI-MS^n

LC-ESI-MSn was used for qualitative analysis of plant extracts and identification of metabolites. An Agilent 6320 Ion Trap mass spectrometer connected to an Agilent 1100 HPLC system (Agilent Tech. Inc., CA) equipped with a diode array detector was utilised. Separation was done with a LUNA 3μ, C18 (2), 100 Å, 150 × 2 mm column (Phenomenex, Aschaffenburg, Germany). The gradient program was as follows: 0–30 min 0–50% B, 30–35 min 50–100% B, 35–50 min 100% B, 50–55 min 100-0% B, 55–65 min 0% B with a flow rate of 0.2 mL/min. Solvent A was water/0.1% formic acid, solvent B methanol/0.1% formic acid. Injection volume was 5 μL. The voltage of the capillary was −3500 V and the end plate was set to −500 V. The capillary exit was 121 V and the Octopole RF amplitude 171 Vpp. The dry gas (N_2) temperature was set to 330 °C at a flow of 9 L/min, nebuliser gas pressure was 30 psi. Tandem MS was carried out using helium as collision gas. Spectra were acquired in the m/z 50–800 range at the Ultra Scan mode. For MS2 spectra ions with 132, 133, 148, 150, 164, 188, 205, 312, 334, 344, 366, 493, 623, and 709 m/z were chosen as precursors. Spectra were analysed in the positive ionization mode. Metabolites were identified by their retention times, mass spectra, and product ion spectra in comparison with the data determined for authentic reference materials. Metabolites were identified by the parameters as stated in Supplemental Table S3.

5.13. Identification of 5HION

5.13.1. General experimental procedure

1D and 2D NMR spectroscopy ^{1}H, ^{1}H–^{1}H COSY, HSQC, HMBC and ^{13}C were performed on an Avance III 500 MHz spectrometer with a CTCI probe (Bruker, Rheinstetten, Germany). Chemical shifts were referenced to the solvent signal of d_3-MeOD (3.31 and 49.0 ppm). Mass spectra of the compounds were measured on a Waters Synapt G2-S HDMS mass spectrometer (Waters, Manchester, UK) coupled to an Acquity UPLC core system (Waters, Milford, MA, USA).

5.13.2. Extraction and isolation of 5HIONG

MeOH extract of Arabidopsis (1 g of *pSur2::Bx1 p35S::Bx2* plants)

was fractionated by means of solid-phase extraction (SPE), thus extract aliquots (200 mg, each) were dissolved in H_2O (3 mL), sonicated for 10 min, membrane filtered, and then loaded onto the top of a C18 ec cartridge (10 g, Chromabond, Macherey-Nagel, Düren, Germany) preconditioned with MeOH, followed by H_2O. Fractionation was performed by flushing the column with decreasing polarity using H_2O and different MeOH/H_2O ratios: H_2O (20 mL; fraction S1), MeOH/H_2O (20/80, v/v; 20 mL; fraction S2), followed by MeOH/H_2O (50/50, v/v; 20 mL; fraction S3), and methanol (20 mL; fraction S4). The fractions S1–S4 were collected, concentrated in a vacuum and freeze-dried. UPLC-ESI-UV-TOF MS analysis revealed the target compound *m/z* 312 to be in fractions S1 and S2. Fractions S1 and S2 were dissolved in H_2O (1 mL) and were chromatographically fractionated on a preparative HPLC system (PrepStar, Varian, Darmstadt, Germany) consisting of two HPLC-pumps (Model SD-1), a two wavelength UV-detector (Prostar 325), fraction collector (Model 701), and equipped with a RP column (phenyl hexyl, 10 × 250 mm, 5 μm; Phenomenex, Aschaffenburg, Germany) as the stationary phase. Monitoring the effluent (4.2 mL/min) at 220 and 270 nm, chromatography was performed starting with a mixture (99/1, v/v) of aqueous HCOOH (0.1% in H_2O) and MeCN for 8 min, the MeCN content was increased to 20% within 25 min and to 50% within 2 min, followed by column washing and re-equilibration. The target compound was collected, concentrated in a vacuum and freeze-dried.

Numbering of the carbons relates to the signal assignment.

Indoline-2-one-5-O-β-D-glucopyranoside (5HIONG): HRESIMS *m/z* 312.1081 $[M+H]^+$ (calcd for $C_{14}H_{18}NO_7$, 312.1083); HRESIMS^e *m/z* 150.0553 (calcd for $C_8H_8NO_2$, 150.0553), *m/z* 122.0604 (calcd for C_7H_8NO, 122.0606); ^{1}H-NMR (500 MHz, d_3-MeOD + D_2O (8/2, v/v), 27 °C, COSY): δ 3.39 [dd, 1H, *J* = 8.9 Hz, H–C (4′)], 3.48 [m, 1H, H–C (2′)], 3.50 [m, 2H, H–C (3’+5′)], 3.57 [s, 2H, H–C (3)], 3.66 [dd, 1H, *J* = 6.0, 12.5 Hz, H–C (6′α)], 3.87 [dd, 1H, *J* = 2.0, 12.5 Hz, H–C (6′β)], 4.87 [d, 1H, *J* = 7.5, H–C (1′)]; 6.90 [d, 1H, *J* = 8.5, H–C (8)], 7.02 [dd, 1H, *J* = 2.5, 8.4, H–C (7)], 7.12 [d, 1H, *J* = 2.4, H–C (5)]; ^{13}C-NMR (125 MHz, d_3-MeOD + D_2O (8/2, v/v), HSQC, HMBC): δ 37.4 [C-3], 62.0 [C-6’], 70.8 [C-4’], 74.5 [C-2’], 77.0 [C-3’], 78.5 [C-5’], 103.0 [C-1’], 111.4 [C-8], 115.6 [C-5], 117.6 [C-7], 127.8 [C-4], 138.8 [C-9], 154.6 [C-6], 180.5 [C-2].

5.13.3. Ultra performance liquid chromatography – electrospray ionization-time-of-flight mass spectrometry (UPLC-ESI-TOF MS)

Aliquots (1 μL) of 5HIONG (0.1 mg/mL, 50% MeCN) were analysed by means of UPLC-ESI-TOF MS on a Waters Synapt G2-S HDMS mass spectrometer (Waters, Manchester, UK) coupled to an Acquity UPLC core system (Waters, Milford, MA, USA) equipped with a 2 × 150 mm, 1.7 μm, BEH C18 column (Waters) consisting of a binary solvent manager, sample manager and column oven. Operated with a flow rate of 0.4 mL/min at 50 °C, the following gradient was used for chromatography: starting with a mixture (1/99, v/v) of aqueous HCO_2H (0.1% in H_2O) and MeCN (0.1% HCO_2H), the MeCN content was increased to 50% within 3 min, to 98% within 1 min, kept constant for 1 min, decreased to 1% within 0.2 min and finally kept constant for 0.8 min at 1%. Scan time for the MS^e method (centroid) was set to 0.1 s. Analyses were performed in the positive ESI and the high resolution mode using the following ion source parameters: capillary voltage +3.0 kV, sampling cone 50 V, source offset 30 V, source temperature 120 °C, desolvation temperature 450 °C, nebuliser 6.5 bar and desolvation gas 850 L/h. Data processing was performed by using MassLynx 4.1 SCN 9.16 (Waters), the elemental composition tool for determining the accurate mass. All data were lock mass corrected on the pentapeptide leucine enkephaline (Tyr-Gly-Gly-Phe-Leu, 556.2771, $[M+H]^+$) in a solution (200 pg/μL) of MeCN/0.1% HCO_2H (1/1, v/v). Scan time for the lock mass was set to 0.3 s, an interval of 15 s and 3 scans to average with a mass window of ±0.3 Da. Calibration of the Synapt G2-S in the range from *m/z* 50 to 1200 was performed using a solution of HCO_2Na (5 mmoL/l) in 2-propanol/H_2O (9/1, v/v). The UPLC and Synapt G2-S systems were operated with MassLynx software (Waters). The collision energy ramp for the high collision energy function was set from 20 to 40 eV inducing fragmentation in the transfer cell.

5.13.4. UPLC-MS/MS quantitation of GDIBOA

Quantitation of the analyte was performed by means of a calibration curve using GDIBOA as analyte and 4-methylumbelliferyl- β-D-glucuronide as internal standard. Standard solutions of GDIBOA (50 μmol, 25 μmol, 15 μmol, 10 μmol, 5 μmol, 2 μmol, 1 μmol, 0.5 μmol, 0.1 μmol, 0.05 μmol, 0.01 μmol in MeOH) and 4-methylumbelliferyl-β-D-glucuronide (4.0 μg/mL in MeOH) were mixed and analysed in triplicates by means of UPLC-MS/MS. Calibration curve was prepared by plotting peak area ratios of analyte to internal standard against concentration ratios of each analyte to the internal standard using linear regression (origin excluded). The equation for the quantifier mass transition obtained was y = 0.00774x-0.00002 (GDIBOA/4-methylumbelliferyl-β-D-glucuronide, $R^2 = 0.98$). Freeze-dried leafs were ground to powder and aliquots (50 mg) were extracted via vortexing (10 s) with MeOH (500 μL) containing the internal standard solution (4 μg/mL), centrifugation (1.5 min, 16.000 g) followed by the extraction with MeOH (500 μL) and centrifugation twice. The combined extracts were evaporated by means of vacuum centrifugation to dryness, then, redissolved in MeOH (100 μL). Mass spectrometric analyses were performed on a Waters Xevo TQ-S mass spectrometer (Waters, Manchester, UK) coupled to an Acquity UPLC i-class core system (Waters, Milford, MA, USA) consisting of a binary solvent manager, sample manager, and column oven. Diluted aliquots (3 μL, 1:100 with MeOH) of prepared samples as well as calibration solutions were injected into the UPLC/MS-MS system equipped with a 2.1 × 150 mm, 1.7 μm, UPLC BEH C18 column (Waters, Manchester, UK). Operated with a flow rate of 0.4 mL/min at a temperature of 50 °C, the following gradient was used for chromatography: starting with a mixture (5/95, v/v, A/B) of aqueous formic acid (0.1% HCOOH) as solvent A and of MeCN (0.1% HCOOH) as solvent B, solvent B was increased to 99% within 3.0 min, kept constant for 0.7 min, decreased within 0.3 min–5%, and followed by re-equilibration on starting conditions for 0.5 min. Measurements were performed using positive electrospray ionization (ESI) and the quantitative calibration mode consisting of the following ion source parameters: capillary voltage +3.0 kV, sampling cone 25 V, source offset 50 V, source temperature 150 °C, desolvation temperature 500 °C, cone gas 150 L/h, desolvation gas 900 L/h, collision gas flow 0.15 mL/min and nebuliser gas flow 7.0 bar. Calibration of the mass spectrometer in the range from *m/z* 40–1963 was performed using a solution of phosphoric acid (0.1% in MeCN). The UPLC Xevo TQ-S system was operated with MassLynx™ 4.1 SCN 813 (Waters), data processing and analysis were performed using TargetLynx (Waters). By means of the multiple reaction monitoring (MRM) mode, the protonated adducts of GDIBOA and (*m/z* 344.2 → qualifier: *m/z* 182.2; quantifier: *m/z* 164.2) 4-methylumbelliferyl-β-D-glucuronide (*m/z* 353.2→ qualifier: *m/z* 105.2; quantifier: *m/z* 175.1) were analysed using the mass transitions (given in brackets) monitored for a duration of 25 ms. ESI^+ mass and product ion spectra were acquired with direct flow infusion using IntelliStart. The MS/MS parameters were tuned for each individual compound, detecting the fragmentation of the $[M+H]^+$ molecular ions into specific product ions after collision with argon.

5.14. Glucosinolate analysis

Glucosinolates analysis was performed with six-week-old rosette leaves. Leaves were analysed triplicates. Rosette leaves were harvested and lyophilised until dryness in freeze temperature. About 20 mg freeze-dried rosette leaves were spiked with 10 μl of 5 mM benzyl-glucosinolate as internal standard and incubated 4 min in 4 mL 70% methanol at 80 °C. Extraction was repeated under the same conditions with 2 mL methanol. About DEAE Sepharose TM fast flow (400 μl per column) was equilibrated with 1 mL of 0,02 M KAC, pH 5.0, and washed with 1 mL H_2O. The combined extracts were applied to the columns, washed twice

with 4 mL H_2O and the columns plugged. 100 µl of 2, 5 mg/mL sulfatase solution were added and incubated overnight. The desulfated glucosinolates were eluted with twice 900 µl H_2O. The eluate was desiccated in the speedvac under at 50 °C, the residues were dissolved in 300 µl H_2O.

HPLC analysis was carried out on a LiChroCART ® 250-4 LiChrospher ® 100 RP-18e (5 µm) column (Merck, Darmstadt) using Dionex 2284 Softron SP2. Analysis was done with the chromatography data system Chromeleon version 6.80, HPLC chromatograms. The UV-vis absorption spectra at 229 nm were analysed. As mobile phases in the analysis H_2O (A) and methanol (B) were used at a flow rate of 1.0 mL/min. Conditions: 0 min, 100% A; 50 min, 40% A; 53 min 0% A; 56 min 0% A; 56,1 min 100% A. The following retention times were obtained for each compound: 3-methyl- sulfinylpropyl- (3-msp) 8,2 min, 4-methylsulfinylbutyl- (4- msb) 10,5 min, 4-methylthiobutyl- (4-mtb) 23,5 min, unmodified indolyl-3-methyl glucosinolate (I3M) 25,8 min, 8-methylsulfinyloctyl- (8- mso) 28,7 min, 4-methoxy I3M (4 M-I3M) 31,0 min, 1-methoxy I3M (1 M-I3M) 36,2 min. The values were normalised according to the dry weight and internal standard.

5.15. Hormone analysis

Plant material (50–250 mg) was placed in a 2 mL bead beater tube (CKMix-2 mL, Bertin Technologies, Montigny-le-Bretonneux, France), filled with ceramic balls (zirconium oxide; mix beads of 1.4 mm and 2.8 mm), an aliquot (20 μL) of a solution of the internal standard salicylic acid-d_4 (2.5 μg/mL) in acetonitrile was added and incubated for 30 min at room temperature. Afterwards ethyl acetate (1 mL) was added. After extractive grinding (3 × 30 s with 40 s breaks; 6000 rpm) using the bead beater (Precellys Homogeniser, Bertin Technologies, Montigny-le-Bretonneux, France) the supernatant was membrane filtered (0.45 μm), evaporated to dryness, resumed in acetonitrile (70 μL) and injected into the LC−MS/MS-system (2 μL).

Liquid Chromatography-Triple Quadrupole Mass Spectrometry (LC−MS/MS). The detection and quantification of phytohormones was performed as described in Chaudhary et al. (2020). Briefly, 6500$^+$ mass spectrometer (Sciex, Darmstadt, Germany) was used to acquire electrospray ionization (ESI) mass spectra and product ion spectra. The MS/MS system was operated in the multiple reaction monitoring (MRM) mode detecting negative and positive ions in the scheduled MRM mode. Negative ions were detected at an ion spray voltage at −4500 V (ESI$^-$) and the following ion source parameters: curtain gas (35 psi), temperature (550 °C), gas 1 (55 psi), gas 2 (65 psi), collision activated dissociation (−3 V), and entrance potential (−10 V). The column oven temperature was adjusted to 40 °C.

For analysis of the plant hormones, the MS/MS parameters were tuned to achieve fragmentation of the [M-H]$^-$ molecular ions into specific product ions: [M-H]$^-$: salicylic acid-d_0 137 → 93 (quantifier) and 137 → 65 (qualifier), salicylic acid-d_4 141 → 97 (quantifier) and 141 → 69 (qualifier); For tuning, acetonitrile/water solutions of the analyte and internal standard were introduced by means of flow injection using a syringe pump. The samples were separated by means of a ExionLC UHPLC (Shimadzu Europa GmbH, Duisburg, Germany) consisting of two LC pump systems ExionLC AD, a ExionLC degasser, a ExionLC AD autosampler, a ExionLC AC column oven – 240 V and a ExionLC controller, and equipped with a 100 × 2.1 mm^2, 100 Å, 1.7 μm, Kinetex F5 column (Phenomenex, Aschaffenburg, Germany). Operated with a flow rate of 0.4 mL/min using 0.1% formic acid in water (v/v) as solvent A and 0.1% formic acid in acetonitrile (v/v) as solvent B, chromatography was performed with the following gradient: 0% B held for 2 min, increased in 1 min–30% B, in 12 min–30% B, increased in 0.5 min–100% B, held 2 min isocratically at 100% B, decreased in 0.5 min to 0% B, held 3 min at 0% B. Data acquisition and instrumental control were performed with Analyst 1.6.3 software (Sciex, Darmstadt, Germany).

5.16. Statistical analysis

All statistical analyses were performed using R 4.0.2 (R Core Team, 2020) and Microsoft Excel 2016. For pairwise comparisons two-tailed Student's t-tests were conducted.

Hormone contents were log transformed and genotypic means were calculated with the R-package emmeans to account for the unbalanced experimental design (Lenth et al., 2021). Tukey's multiple-comparison test was used to evaluate statistical significance.

Differences in relative gene expression were analysed by one-way ANOVA followed by Tukey's test to evaluate the statistical significance of the differences in means. P-values < 0.05 were considered significant.

Declaration of competing interest

The authors declare that they have no known competing financial interests or personal relationships that could have appeared to influence the work reported in this paper.

Acknowledgements

We are grateful to Erich Glawischnig for the help with the analysis of GLS and for T-DNA mutant seeds and Ramon Torres Ruiz for assistance in microscopy. We thank Michael Gigl for LC-MS additional hormone analyses. We appreciate the work of Henriette Leicher and Shuyao Chen on analysis of Arabidopsis transgenics. Corina Vlot and Marion Wenig are gratefully acknowledged for providing seeds, experimental help and the fruitful scientific discussions. We thank Anton Schäffner for providing NahG seed.

This work was supported by a grant from the Deutsche Forschungsgemeinschaft (SFB924 to MF).

Appendix A. Supplementary data

Supplementary data to this article can be found online at https://doi.org/10.1016/j.phytochem.2021.112947.

Author contributions

M.F., A.G.,A.A. conceived the project and original research plans. A. A. performed and analysed the experiments. T.H., T.D.S, R.H., W.S., C.D. designed and performed metabolite analysis. L.Z. and S.L. generated transgenic plants used in the analysis and analysed auxin and GLS pattern, T.L. contributed with statistical analysis. C–C.S. enabled the set-up of some experiments. M.F. and A.A. wrote the article with contributions of all authors.

References

Beckett, A.H., Morton, D.M., 1966. The metabolism of oxindole and related compounds. Biochem. Pharmacol. 15, 937–946. https://doi.org/10.1016/0006-2952(66)90170-5.

Brader, G., Mikkelsen, M.D., Halkier, B.A., Tapio Palva, E., 2006. Altering glucosinolate profiles modulates disease resistance in plants. Plant J. 46, 758–767. https://doi.org/10.1111/j.1365-313X.2006.02743.x.

Bravo, H.R., Copaja, S.V., Lazo, W., 1997. Antimicrobial activity of natural 2-benzoxazolinones and related derivatives. J. Agric. Food Chem. 45, 3255–3257. https://doi.org/10.1021/jf9608581.

Bravo, H.R., Lazo, W., 1996. Antialgal and antifungal activity of natural hydroxamic acids and related compounds. J. Agric. Food Chem. 44, 1569–1571. https://doi.org/10.1021/jf950345e.

Campos, F., Atkinson, J., Arnason, J.T., Philogène, B.J.R., Morand, P., Werstiuk, N.H., Timmins, G., 1989. Toxicokinetics of 2,4-dihydroxy-7-methoxy-1,4-benzoxazin-3-one (DIMBOA) in the European corn borer, Ostrinia nubilalis (Hübner). J. Chem. Ecol. 15, 1989–2001. https://doi.org/10.1007/BF01207432.

Cane, A., Tournaire, M.-C., Barritault, D., Crumeyrolle-Arias, M., 2000. The endogenous oxindoles 5-hydroxyoxindole and isatin are antiproliferative and proapoptotic. Biochem. Biophys. Res. Commun. 276, 379–384. https://doi.org/10.1006/bbrc.2000.3477.

Chapple, C., 1998. Molecular-genetic analysis of plant cytochrome P450-dependent monooxygenases. Annu. Rev. Plant Physiol. Plant Mol. Biol. 49, 311–343. https://doi.org/10.1146/annurev.arplant.49.1.311.

Chaudhary, A., Chen, X., Gao, J., Leśniewska, B., Hammerl, R., Dawid, C., Schneitz, K., 2020. The Arabidopsis receptor kinase STRUBBELIG regulates the response to cellulose deficiency. PLOS Genetics 16, e1008433. https://doi.org/10.1371/journal.pgen.1008433.

Copaja, S.V., Villarroel, E., Bravo Héctor, R., Pizarro, L., Argandoñ Víctor, H., 2006. Hydroxamic acids in secale cereale L. And the relationship with their antifeedant and allelopathic properties. Z. Naturforsch. Sect. C 61, 670. https://doi.org/10.1515/znc-2006-9-1010.

Crumeyrolle-Arias, M., Tournaire, M.-C., Rabot, S., Malpaux, B., Thiéry, J.-C., 2008. 5-hydroxyoxindole, an indole metabolite, is present at high concentrations in brain. J. Neurosci. Res. 86, 202–207. https://doi.org/10.1002/jnr.21475.

de Carolis, E., de Luca, V., 1994. 2-Oxoglutarate-dependent dioxygenase and related enzymes: biochemical characterization. Phytochemistry 36, 1093–1107. https://doi.org/10.1016/S0031-9422(00)89621-1.

Dick, R., Rattei, T., Haslbeck, M., Schwab, W., Gierl, A., Frey, M., 2012. Comparative analysis of benzoxazinoid biosynthesis in monocots and dicots: independent recruitment of stabilization and activation functions. Plant Cell 24, 915–928. https://doi.org/10.1105/tpc.112.096461.

Dutartre, L., Hilliou, F., Feyereisen, R., 2012. Phylogenomics of the benzoxazinoid biosynthetic pathway of Poaceae: gene duplications and origin of the Bx cluster. BMC Evol. Biol. 12, 64. https://doi.org/10.1186/1471-2148-12-64.

Frey, M., Chomet, P., Glawischnig, E., Stettner, C., Grün, S., Winklmair, A., Eisenreich, W., Bacher, A., Meeley, R.B., Briggs, S.P., Simcox, K., Gierl, A., 1997. Analysis of a chemical plant defense mechanism in grasses. Science 277, 696–699. https://doi.org/10.1126/science.277.5326.696.

Frey, M., Reinecke, J., Grant, S., Saedler, H., Gierl, A., 1990. Excision of the En/Spm transposable element of Zea mays requires two element-encoded proteins. EMBO J. 9, 4037–4044. https://doi.org/10.1002/j.1460-2075.1990.tb07625.x.

Frey, M., Schullehner, K., Dick, R., Fiesselmann, A., Gierl, A., 2009. Benzoxazinoid biosynthesis, a model for evolution of secondary metabolic pathways in plants. Phytochemistry 70, 1645–1651. https://doi.org/10.1016/j.phytochem.2009.05.012.

Frey, M., Stettner, C., Paré, P.W., Schmelz, E.A., Tumlinson, J.H., Gierl, A., 2000. An herbivore elicitor activates the gene for indole emission in maize. Proc. Natl. Acad. Sci. Unit. States Am. 97, 14801–14806. https://doi.org/10.1073/pnas.260499897.

Grün, S., Frey, M., Gierl, A., 2005. Evolution of the indole alkaloid biosynthesis in the genus Hordeum: distribution of gramine and DIBOA and isolation of the benzoxazinoid biosynthesis genes from Hordeum lechleri. Phytochemistry 66, 1264–1272. https://doi.org/10.1016/j.phytochem.2005.01.024.

Halkier, B.A., Gershenzon, J., 2006. Biology and biochemistry of glucosinolates. Annu. Rev. Plant Biol. 57, 303–333. https://doi.org/10.1146/annurev.arplant.57.032905.105228.

Halkier, B.A., Møller, B.L., 1989. Biosynthesis of the cyanogenic glucoside dhurrin in seedlings of sorghum bicolor (L.) moench and partial purification of the enzyme system involved. Plant Physiol 90, 1552. https://doi.org/10.1104/pp.90.4.1552.

Handrick, V., Robert, C.A.M., Ahern, K.R., Zhou, S., Machado, R.A.R., Maag, D., Glauser, G., Fernandez-Penny, F.E., Chandran, J.N., Rodgers-Melnik, E., Schneider, B., Buckler, E.S., Boland, W., Gershenzon, J., Jander, G., Erb, M., Köllner, T.G., 2016. Biosynthesis of 8-O-methylated benzoxazinoid defense compounds in maize. Plant Cell 28, 1682. https://doi.org/10.1105/tpc.16.00065.

Hartmann, T., 2007. From waste products to ecochemicals: fifty years research of plant secondary metabolism. Phytochemistry 68, 2831–2846. https://doi.org/10.1016/j.phytochem.2007.09.017.

Hietala, P.K., Virtanen, A.I., 1960. Precursors of benzoxazolinone in rye plants. II. Precursor I, the Glucoside. Acta Chem. Scand. 14, 502–504. https://doi.org/10.3891/acta.chem.scand.14-0502.

Horowitz, N.H., 1945. On the evolution of biochemical syntheses. Proc. Natl. Acad. Sci. U.S.A. 31, 153–157. https://doi.org/10.1073/pnas.31.6.153.

Huffaker, A., Pearce, G., Veyrat, N., Erb, M., Turlings, T.C.J., Sartor, R., Shen, Z., Briggs, S.P., Vaughan, M.M., Alborn, H.T., Teal, P.E.A., Schmelz, E.A., 2013. Plant elicitor peptides are conserved signals regulating direct and indirect antiherbivore defense. Proc. Natl. Acad. Sci. Unit. States Am. 110, 5707–5712. https://doi.org/10.1073/pnas.1214668110.

Inoue, S., Morita, R., Minami, Y., 2021. An indigo-producing plant, Polygonum tinctorium, possesses a flavin-containing monooxygenase capable of oxidizing indole. Biochem. Biophys. Res. Commun. 534, 199–205. https://doi.org/10.1016/j.bbrc.2020.11.112.

Jonczyk, R., Schmidt, H., Osterrieder, A., Fiesselmann, A., Schullehner, K., Haslbeck, M., Sicker, D., Hofmann, D., Yalpani, N., Simmons, C., Frey, M., Gierl, A., 2008. Elucidation of the final reactions of DIMBOA-glucoside biosynthesis in maize: characterization of Bx6 and Bx7. Plant Physiol 146, 1053–1063. https://doi.org/10.1104/pp.107.111237.

Jones, P., Vogt, T., 2001. Glycosyltransferases in secondary plant metabolism: tranquilizers and stimulant controllers. Planta 213, 164–174. https://doi.org/10.1007/s004250000492.

Jørgensen, K., Rasmussen, A.V., Morant, M., Nielsen, A.H., Bjarnholt, N., Zagrobelny, M., Bak, S., Møller, B.L., 2005. Metabolon formation and metabolic channeling in the biosynthesis of plant natural products. Curr. Opin. Plant Biol. 8, 280–291. https://doi.org/10.1016/j.pbi.2005.03.014.

Kim, T.-W., Chang, S.C., Lee, J.S., Hwang, B., Takatsuto, S., Yokota, T., Kim, S.-K., 2004. Cytochrome P450-catalyzed brassinosteroid pathway activation through synthesis of castasterone and brassinolide in Phaseolus vulgaris. Phytochemistry 65, 679–689. https://doi.org/10.1016/j.phytochem.2004.01.007.

Kleinboelting, N., Huep, G., Kloetgen, A., Viehoever, P., Weisshaar, B., 2011. GABI-Kat SimpleSearch: new features of the Arabidopsis thaliana T-DNA mutant database. Nucleic Acids Res. 40, D1211–D1215. https://doi.org/10.1093/nar/gkr1047.

Klun, J.A., Guthrie, W.D., Hallauer, A.R., Russell, W.A., 1970. Genetic nature of the concentration of 2,4-dihydroxy-7-methoxy 2H-l,4-benzoxazin- 3(4H)-one and resistance to the European corn borer in a diallel set of eleven maize Inbreds 1. Crop Sci. 10, 87–90. https://doi.org/10.2135/cropsci1970.0011183X001000010032x.

Klun, J.A., Tipton, C.L., Brindley, T.A., 1967. 2,4-Dihydroxy-7-methoxy-1,4-benzoxazin-3-one (DIMBOA), an active agent in the resistance of maize to the European corn Borer 123. J. Econ. Entomol. 60, 1529–1533. https://doi.org/10.1093/jee/60.6.1529.

Knudsen, C., Gallage, N.J., Hansen, C.C., Møller, B.L., Laursen, T., 2018. Dynamic metabolic solutions to the sessile life style of plants. Nat. Prod. Rep. 35, 1140–1155. https://doi.org/10.1039/C8NP00037A.

Laursen, T., Borch, J., Knudsen, C., Bavishi, K., Torta, F., Martens, H.J., Silvestro, D., Hatzakis, N.S., Wenk, M.R., Dafforn, T.R., Olsen, C.E., Motawia, M.S., Hamberger, B., Møller, B.L., Bassard, J.-E., 2016. Characterization of a dynamic metabolon producing the defense compound dhurrin in sorghum. Science 354, 890. https://doi.org/10.1126/science.aag2347.

Laursen, T., Møller, B.L., Bassard, J.-E., 2015. Plasticity of specialized metabolism as mediated by dynamic metabolons. Trends Plant Sci. 20, 20–32. https://doi.org/10.1016/j.tplants.2014.11.002.

Lee, S., Kim, S.-G., Park, C.-M., 2010. Salicylic acid promotes seed germination under high salinity by modulating antioxidant activity in Arabidopsis. New Phytol. 188, 626–637. https://doi.org/10.1111/j.1469-8137.2010.03378.x.

Lenk, S., 2015. Transfer of the DIBOA biosynthesis pathway from maize to Arabidopsis thaliana. In: Lehrstuhl für Genetik, PhD. Technische Universität München, Freising, p. 81. http://mediatum.ub.tum.de/doc/1238084/document.pdf.

Lenth, R.V., Beuerkner, P., Herve, M., Love, J., Riebl, H., Singmann, H., 2021. Emmeans" Package for R. https://CRAN.R-project.org/package=emmeans.

Li, Y., Zhang, Z., Jia, Y., Shen, Y., He, H., Fang, R., Chen, X., Hao, X., 2008. 3-Acetonyl-3-hydroxyoxindole: a new inducer of systemic acquired resistance in plants. Plant Biotechnol. J. 6, 301–308. https://doi.org/10.1111/j.1467-7652.2008.00322.x.

Long, B.J., Dunn, G.M., Routley, D.G., 1975. Relationship of hydroxamic acid content in maize and resistance to northern corn leaf blight. Crop Sci. 15 https://doi.org/10.2135/cropsci1975.0011183X001500030015x cropsci1975.0011183X001500030015x.

Luichtl, M., Fiesselmann, B.S., Matthes, M., Yang, X., Peis, O., Brunner, A., Torres-Ruiz, R.A., 2013. Mutations in the Arabidopsis RPK1 gene uncouple cotyledon anlagen and primordia by modulating epidermal cell shape and polarity. Biology Open 2, 1093–1102. https://doi.org/10.1242/bio.20135991.

Maier, W., Schumann, B., Gröger, D., 1990. Biosynthesis of indoxyl derivatives in Isatis tinctoria and Polygonum tinctorium. Phytochemistry 29, 817–819. https://doi.org/10.1016/0031-9422(90)80025-C.

Meihls, L.N., Handrick, V., Glauser, G., Barbier, H., Kaur, H., Haribal, M.M., Lipka, A.E., Gershenzon, J., Buckler, E.S., Erb, M., Köllner, T.G., Jander, G., 2013. Natural variation in maize aphid resistance is associated with 2,4-dihydroxy-7-methoxy-1,4-benzoxazin-3-one glucoside methyltransferase activity. Plant Cell 25, 2341–2355. https://doi.org/10.1105/tpc.113.112409.

Mlotshwa, S., Pruss, G.J., Gao, Z., Mgutshini, N.L., Li, J., Chen, X., Bowman, L.H., Vance, V., 2010. Transcriptional silencing induced by Arabidopsis T-DNA mutants is associated with 35S promoter siRNAs and requires genes involved in siRNA-mediated chromatin silencing. Plant J. 64, 699–704. https://doi.org/10.1111/j.1365-313X.2010.04358.x.

Møldrup, M.E., Geu-Flores, F., de Vos, M., Olsen, C.E., Sun, J., Jander, G., Halkier, B.A., 2012. Engineering of benzylglucosinolate in tobacco provides proof-of-concept for dead-end trap crops genetically modified to attract Plutella xylostella (diamondback moth). Plant Biotechnol. J. 10, 435–442. https://doi.org/10.1111/j.1467-7652.2011.00680.x.

Møldrup, M.E., Geu-Flores, F., Olsen, C.E., Halkier, B.A., 2011. Modulation of sulfur metabolism enables efficient glucosinolate engineering. BMC Biotechnol. 11, 12. https://doi.org/10.1186/1472-6750-11-12.

Niculaes, C., Abramov, A., Hannemann, L., Frey, M., 2018. Plant protection by benzoxazinoids—recent insights into biosynthesis and function. Agronomy 8. https://doi.org/10.3390/agronomy8080143.

Nikus, J., Daniel, G., Jonsson, L.M.V., 2001. Subcellular localization of β-glucosidase in rye, maize and wheat seedlings. Physiol. Plantarum 111, 466–472. https://doi.org/10.1034/j.1399-3054.2001.1110406.x.

Nintemann, S.J., Hunziker, P., Andersen, T.G., Schulz, A., Burow, M., Halkier, B.A., 2018. Localization of the glucosinolate biosynthetic enzymes reveals distinct spatial patterns for the biosynthesis of indole and aliphatic glucosinolates. Physiol. Plantarum 163, 138–154. https://doi.org/10.1111/ppl.12672.

Nomura, T., Ishihara, A., Yanagita, R.C., Endo, T.R., Iwamura, H., 2005. Three genomes differentially contribute to the biosynthesis of benzoxazinones in hexaploid wheat. Proc. Natl. Acad. Sci. U.S.A. 102, 16490. https://doi.org/10.1073/pnas.0505156102.

Nützmann, H.-W., Huang, A., Osbourn, A., 2016. Plant metabolic clusters – from genetics to genomics. New Phytol. 211, 771–789. https://doi.org/10.1111/nph.13981.

Pentzold, S., Zagrobelny, M., Rook, F., Bak, S., 2014. How insects overcome two-component plant chemical defence: plant β-glucosidases as the main target for herbivore adaptation. Biol. Rev. 89, 531–551. https://doi.org/10.1111/brv.12066.

Petersen, A., Wang, C., Crocoll, C., Halkier, B.A., 2018. Biotechnological approaches in glucosinolate production. J. Integr. Plant Biol. 60, 1231–1248. https://doi.org/10.1111/jipb.12705.

Pluhařová, K., Leontovyčová, H., Stoudková, V., Pospíchalová, R., Maršík, P., Klouček, P., Starodubtseva, A., Iakovenko, O., Krčková, Z., Valentová, O.,

Burketová, L., Janda, M., Kalachova, T., 2019. “Salicylic acid mutant collection” as a tool to explore the role of salicylic acid in regulation of plant growth under a changing environment. Int. J. Mol. Sci. 20, 6365. https://doi.org/10.3390/ijms20246365.

Rademacher, W., Temple-smith, K.E., Griggs, D.L., Hedden, P., 1992. The mode of action of acylcyclohexanediones — a new type of growth retardant. In: Karssen, C.M., v L L C, Vreugdenhil, D. (Eds.), Progress in Plant Growth Regulation, Current Plant Science and Biotechnology in Agriculture, vol. 13. Springer, Dordrecht, pp. 571–577. https://doi.org/10.1007/978-94-011-2458-4_68.

Rajjou, L., Belghazi, M., Huguet, R., Robin, C., Moreau, A., Job, C., Job, D., 2006. Proteomic investigation of the effect of salicylic acid on arabidopsis seed germination and establishment of early defense mechanisms. Plant Physiol 141, 910. https://doi.org/10.1104/pp.106.082057.

R Core Team (2020). R: A language and environment for statistical computing. R Foundation for Statistical Computing, Vienna, Austria. URL https://www.R-project.org/.

Rice, C.P., Park, Y.B., Adam, F., Abdul-Baki, A.A., Teasdale, J.R., 2005. Hydroxamic acid content and toxicity of rye at selected growth stages. J. Chem. Ecol. 31, 1887–1905. https://doi.org/10.1007/s10886-005-5933-6.

Richter, A., Powell, A.F., Mirzaei, M., Wang, L.J., Movahed, N., Miller, J.K., Piñeros, M. A., Jander, G., 2021. Indole-3-glycerolphosphate synthase, a branchpoint for the biosynthesis of tryptophan, indole, and benzoxazinoids in maize. Plant J. 106, 245–257. https://doi.org/10.1111/tpj.15163.

Šašek, V., Janda, M., Delage, E., Puyaubert, J., Guivarc’h, A., López Maseda, E., Dobrev, P.I., Caius, J., Bóka, K., Valentová, O., Burketová, L., Zachowski, A., Ruelland, E., 2014. Constitutive salicylic acid accumulation in pi4kIIIβ1β2 Arabidopsis plants stunts rosette but not root growth. New Phytol. 203, 805–816. https://doi.org/10.1111/nph.12822.

Schullehner, K., Dick, R., Vitzthum, F., Schwab, W., Brandt, W., Frey, M., Gierl, A., 2008. Benzoxazinoid biosynthesis in dicot plants. Phytochemistry 69, 2668–2677. https://doi.org/10.1016/j.phytochem.2008.08.023.

Schulz, M., Filary, B., Kühn, S., Colby, T., Harzen, A., Schmidt, J., Sicker, D., Hennig, L., Hofmann, D., Disko, U., Anders, N., 2016. Benzoxazolinone detoxification by N-Glucosylation: the multi-compartment-network of Zea mays L. Plant Signal. Behav. 11, e1119962 https://doi.org/10.1080/15592324.2015.1119962.

Schulz, M., Marocco, A., Tabaglio, V., Macias, F.A., Molinillo, J.M., 2013. Benzoxazinoids in rye allelopathy - from discovery to application in sustainable weed control and organic farming. J. Chem. Ecol. 39, 154–174. https://doi.org/10.1007/s10886-013-0235-x.

Scott, I.M., Clarke, S.M., Wood, J.E., Mur, L.A.J., 2004. Salicylate accumulation inhibits growth at chilling temperature in arabidopsis. Plant Physiol 135, 1040. https://doi.org/10.1104/pp.104.041293.

Staley, J.T., Stewart-Jones, A., Poppy, G.M., Leather, S.R., Wright, D.J., 2009. Fertilizer affects the behaviour and performance of Plutella xylostella on brassicas. Agric. For. Entomol. 11, 275–282. https://doi.org/10.1111/j.1461-9563.2009.00432.x.

Stelpflug, S.C., Sekhon, R.S., Vaillancourt, B., Hirsch, C.N., Buell, C.R., de Leon, N., Kaeppler, S.M., 2016. An expanded maize gene expression atlas based on RNA sequencing and its use to explore root development. Plant Genome 9. https://doi.org/10.3835/plantgenome2015.04.0025.

Tattersall, D.B., Bak, S., Jones, P.R., Olsen, C.E., Nielsen, J.K., Hansen, M.L., Høj, P.B., Møller, B.L., 2001. Resistance to an herbivore through engineered cyanogenic glucoside synthesis. Science 293, 1826–1828. https://doi.org/10.1126/science.1062249.

Urban, P., Cullin, C., Pompon, D., 1990. Maximizing the expression of mammalian cytochrome P-450 monooxygenase activities in yeast cells. Biochimie 72, 463–472. https://doi.org/10.1016/0300-9084(90)90070-w.

Vlot, A.C., Dempsey, D.M.A., Klessig, D.F., 2009. Salicylic acid, a multifaceted hormone to combat disease. Annu. Rev. Phytopathol. 47, 177–206. https://doi.org/10.1146/annurev.phyto.050908.135202.

Vogelmann, K., Drechsel, G., Bergler, J., Subert, C., Philippar, K., Soll, J., Engelmann, J. C., Engelsdorf, T., Voll, L.M., Hoth, S., 2012. Early senescence and cell death in arabidopsis saul 1 mutants involves the PAD4-dependent salicylic acid pathway. Plant Physiol 159, 1477–1487. https://doi.org/10.1104/pp.112.196220.

von Rad, U., Hüttl, R., Lottspeich, F., Gierl, A., Frey, M., 2001. Two glucosyltransferases are involved in detoxification of benzoxazinoids in maize. Plant J. 28, 633–642. https://doi.org/10.1046/j.1365-313x.2001.01161.x.

Wink, M., 2003. Evolution of secondary metabolites from an ecological and molecular phylogenetic perspective. Phytochemistry 64, 3–19. https://doi.org/10.1016/S0031-9422(03)00300-5.

Wink, M., Waterman, P.G., 1998. Chemotaxonomy in relation to molecular phylogeny of plants. Biochem. Plant Second. Metabol. 2, 300–341. https://doi.org/10.1002/9781119312994.apr0017.

Winkel, B.S.J., 2004. Metabolic channeling IN plants. Annu. Rev. Plant Biol. 55, 85–107. https://doi.org/10.1146/annurev.arplant.55.031903.141714.

Winter, D., Vinegar, B., Nahal, H., Ammar, R., Wilson, G.V., Provart, N.J., 2007. An "Electronic Fluorescent Pictograph" browser for exploring and analyzing large-scale biological data sets. PloS One 2, 718. https://doi.org/10.1371/journal.pone.0000718.

Woody, S.T., Austin-Phillips, S., Amasino, R.M., Krysan, P.J., 2007. The WiscDsLox T-DNA collection: an arabidopsis community resource generated by using an improved high-throughput T-DNA sequencing pipeline. J. Plant Res. 120, 157–165. https://doi.org/10.1007/s10265-006-0048-x.

Yang, L., Zhang, Y., Guan, R., Li, S., Xu, X., Zhang, S., Xu, J., 2020. Co-regulation of indole glucosinolates and camalexin biosynthesis by CPK5/CPK6 and MPK3/MPK6 signaling pathways. J. Integr. Plant Biol. 62, 1780–1796. https://doi.org/10.1111/jipb.12973.

Zhang, Y., Fernie, A.R., 2021. Metabolons, enzyme–enzyme assemblies that mediate substrate channeling, and their roles in plant metabolism. Plant Commun. 2, 100081. https://doi.org/10.1016/j.xplc.2020.100081.